

# CHALMERS



## Filtration Efficiency of Intermediate Ventilation Air filters on Ultrafine and Submicron Particles

A laboratory test on new full-scale filter modules

MARÍA DÍEZ MAROTO

Department of Energy and Environment  
*Division of Building Services Engineering*  
CHALMERS UNIVERSITY OF TECHNOLOGY  
Göteborg, Sweden 2011  
Master's Thesis 2011:14



MASTER'S THESIS 2011:14

Filtration Efficiency of Intermediate  
Ventilation Air filters on Ultrafine and  
Submicron Particles

A laboratory test on new full-scale filter modules

MARÍA DÍEZ MAROTO

Department of Civil and Environmental Engineering  
*Division of Building Services Engineering*

CHALMERS UNIVERSITY OF TECHNOLOGY

Göteborg, Sweden 2011

Filtration efficiency of intermediate ventilation air filters on ultrafine and submicron particles

A laboratory test on new full-scale filter modules

MARÍA DÍEZ MAROTO

© MARÍA DÍEZ MAROTO, 2011

Master's Thesis 2011:14

Department of Civil and Environmental Engineering

Division of Building Services Engineering

Chalmers University of Technology

SE-412 96 Göteborg

Sweden

Telephone: + 46 (0)31-772 1000

Department of Civil and Environmental Engineering  
Göteborg, Sweden 2011

Filtration efficiency of intermediate ventilation air filters on ultrafine and submicron particles

A laboratory test on new full-scale filter modules

MARÍA DÍEZ MAROTO

Department of Civil and Environmental Engineering

Division of Building Services Engineering

Chalmers University of Technology

## **Abstract**

A number of recent epidemiological studies have addressed the association of mortality or morbidity of urban populations with ambient submicron and ultrafine particle concentrations. Evaluating the filtration efficiency of intermediate filters on submicron and ultrafine particles is motivated by increasing public concern on indoor air quality in commercial and residential buildings.

The present study is focused on filtration efficiency testing of full-scale fibrous filters of the intermediate (fine) filter classes F5-F9. Special attention has been paid to submicron and ultrafine particles, in experiments conducted in the laboratory of Building Services Engineering, Chalmers University of Technology. A Scanning Mobility Particle Sizer (SMPS) spectrometer was utilized in the test process. The filters were challenged by DEHS aerosol and NaCl aerosol. The tested intermediate bag filter modules are commonly applied, not only in Sweden, but also internationally.

This study systematically researches the filtration efficiency of new intermediate ventilation air filters on submicron and ultrafine particles under the standard test conditions specified in the European standard EN779. It provides important reference data to evaluate the protection capacity of intermediate filters to submicron and ultrafine particles. Furthermore, the study also investigates the influence of air flow rate, filter material, and challenge aerosol on the test results. A separate set of tests was conducted to study the influence from using a neutralizer in order to change the electrostatic properties of the aerosol. The investigation is intended to provide background information when discussing possible improvements of the current standards for filter testing and classification.

### **Key words:**

Filtration efficiency; Particle filters; Ultrafine particles; Submicron particles; Pressure drop; Ventilation.



# Acknowledgement

I would like to acknowledge all the people that made possible the realization of the thesis. This master thesis has been carried out under the supervision of M.Sc. Bingbing Shi. I would like to thank her for her useful help during the experiments and for her important guidance during all the semester.

I would also like to express my gratitude to Assoc. Professor Lars Ekberg whose help and support led to a better understanding of the experiments.

I have to thank Eng. Håkan Larsson for his useful help in the laboratory. Without his advice about the instruments and the test-rig the experiments would have been tougher.

Finally, deepest gratitude to all the companies that provided us the necessary instruments for carrying out the experiments. These companies are TOPAS, TSI, Academic hus AB, Camfil and Vokes Air/Scandfilter.

Göteborg  
2011-06-19

María Díez Maroto



# Contents

ABSTRACT	I
ACKNOWLEDGEMENT	III
CONTENTS	V
SYMBOLS, SUBSCRIPTS, SUPERSSCRIPTS, DEFINITIONS AND ABBREVIATIONS	VII
1 INTRODUCTION	1
1.1 Background	1
1.2 Health effect	1
1.2.1 Submicron and ultrafine particles	1
1.2.2 Deposition in respiratory system	2
1.2.3 Sick-building syndrome	4
1.3 Purpose and scope of the study	4
1.4 Outline of the report	4
1.5 Methodology and limitations	5
2 AIR FILTRATION	7
2.1 Filtration efficiency	7
2.2 Criteria of filter selection	8
2.2.1 Filter class in standards	8
2.2.2 Pressure drop	9
2.3 Filters	10
2.3.1 Fibrous filters	10
2.3.2 High Efficiency Particulate Air filter	11
2.4 Problems of filter application	12
2.4.1 Increase of pressure drop	12
2.4.2 By-products from used filters	13
2.4.3 Reduced efficiency of charged synthetic filters	13
2.4.4 Bypass of air flow	13
2.5 Deposition mechanisms	14
2.6 Power consumption	17
2.7 Costs	17
3 TESTS PLANNING	19
3.1 Experimental instruments	19
3.1.1 Ultrafine particle counter	19
3.1.2 Air velocity and pressure differential measurements	20
3.1.3 Atomizer aerosol generator	21
3.1.4 Scanning Mobility Particle Sizer spectrometer	22
3.1.5 Neutralizer	24

3.2	Qualification of test-rig	25
3.2.1	Uniformity of the air velocity	26
3.2.2	Aerosol uniformity in the test-rig	27
3.2.3	Particle counter zero test	27
3.2.4	Particle counter overload test	27
3.2.5	100% efficiency test	28
3.2.6	Zero % efficiency test	28
3.2.7	Aerosol generator stability	28
3.2.8	Over-pressure checking	28
4	EXPERIMENTAL RESULTS	31
4.1	Pressure drop	32
4.2	Filtration efficiency	34
4.2.1	Filter classes summary	36
4.2.2	Air flow influence	38
4.2.3	Filter media influence	39
4.3	Neutralizer influence	41
4.3.1	Glass fiber filters	41
4.3.2	Charged Synthetic filters	42
4.3.3	Nano-fiber filters	44
4.4	Aerosol influence	45
5	DISCUSSION AND CONCLUSIONS	47
6	FUTURE WORKS	49
7	REFERENCES	51
8	APPENDIX	55
8.1	Calibration of the filter test-rig	55
8.1.1	Air velocity uniformity in the test duct	55
8.1.2	Aerosol uniformity in the test duct	58
8.1.3	Maximum aerosol concentrations in the experiments	59
8.1.4	Zero % efficiency test	60
8.1.5	Aerosol generator stability	60
8.1.6	Filter test-rig under over-pressure	61
8.2	Standard deviation methods	61
8.3	Additional results	62

# Symbols, subscripts, superscripts, definitions and abbreviations

## Symbols

### Latin letters

$A$	Area; $m^2$
$C$	Cost
$C_{down}$	Concentration downstream
$C_{down-background}$	Background concentration downstream
$C_{up}$	Concentration upstream
$C_{up-background}$	Background concentration upstream
$E$	Filtration efficiency
$E_D$	Diffusion efficiency
$E_{DR}$	Interception of the diffusing particles efficiency
$E_G$	Gravitational settling efficiency
$E_I$	Inertial impaction efficiency
$E_R$	Interception efficiency
$e$	Price of the electricity
$H$	Height
$h$	Hours
$L$	Length
$N$	Number
$P$	Penetration
$\dot{Q}$	Volumetric flow rate; $m^3/s$
$U_0$	Air velocity
$U$	Air velocity inside the filter
$V$	Air velocity through the filter medium
$W$	Power
$W_e$	Electrical power

### Greek letters

$\Delta p$	Pressure drop
$\delta$	Standard deviation
$\eta_m$	Motor efficiency
$\eta_T$	Fan total efficiency
$\mu$	Mean value

## Abbreviations

AHU	Air Handling Unit
ASHRAE	American Society of Heating, Refrigerating and Air-Conditioning Engineers, Inc
ANSI	American National Standards Institute
CL	Concentration Limit
CV	Coefficient of Variation
CS	Charged Synthetic
CPC	Condensation Particle Counter
DMA	Differential Mobility Analyzer
DNA	Deoxyribonucleic Acid
GF	Glass Fiber
HVAC	Heat, Ventilating and Air Conditioning
HEPA	High Efficiency Particulate Air
IAQ	Indoor Air Quality
ICRP	International Commission on Radiological Protection
MERV	Minimum Efficiency Reporting Value
MPPS	Most Penetrating Particle Size
OPCs	Optical Particle Counters
PM	Particulate Matter
RSD	Relative Standard Deviation
SD	Standard Deviation
SMPS	Scanning Mobility Particle Sizer
SBS	Sick-building symptoms
UFPs	Ultrafine Particles
ULPA	Ultra Low Penetration Air

# 1 Introduction

## 1.1 Background

People spend around 90% of their time indoors; hence it is important to have a good Indoor Air Quality (IAQ). Indoor air quality depends on the amount of pollutants in the air that can be annoying or harm the people that occupy the room or can damage objects. Air pollutants can harm people's health influencing the occurrence of infectious respiratory illnesses and allergy. These pollutants can be gaseous or particulate, which are formed in different ways and behave differently in the air. Ultrafine particles (UFPs) and submicron particles are of special importance among these air pollutants.

Submicron particles are particles with diameters between 0.01  $\mu\text{m}$  and 1  $\mu\text{m}$ . From a health standpoint, these particles are often judged as being of great concern. This size range is typical of tobacco smoke and radon progeny (daughters) in indoor aerosols.

UFPs are particles with diameters less than 100 nm, which have high penetration rate in people's respiratory system. Due to their small size they are related to DNA oxidation which may cause cancer and pulmonary and cardiovascular diseases.

Particle filters are commonly used to remove air pollutants in buildings and therefore improve IAQ. They are used in most commercial buildings and some residential buildings under high air flow rates. Initially, particle filters were used to protect HVAC (Heating, Ventilating and Air Conditioning) equipment.

Filtration efficiency defines the ability with which a filter removes airborne particles. Efficiency varies with particle size among other variables; the size range where the efficiency reaches its minimum is called most penetrating particle size (MPPS).

Achieving a high efficiency is an important goal in order to avoid adverse effects, such as those mentioned below.

## 1.2 Health effect

### 1.2.1 Submicron and ultrafine particles

Submicron particles have high number density, great ability to penetrate deep into the lungs and are enriched in toxic trace compounds. These characteristics are the reason why the inhalation of submicron particles has dangerous health effects.

UFPs are abundant in particle concentration but have a small contribution to particle mass. The results of different experiments show that biologic effects of UFPs may occur even at low exposure and, as UFPs are ubiquitous, exposure is unavoidable.

UFPs are dangerous due to their small particle size, chemical composition and large surface area which makes them able to cause inflammation (because they generate reactive oxygen species) and transfer to the circulation [28-30]. Experimental studies have shown that UFPs are also related to DNA oxidation (maybe due to the interaction of UFPs in the circulation with circulating mononuclear cells), but apparently do not cause strand breaks [31-36]. This DNA oxidation is related to

cancer and pulmonary and cardiovascular diseases [43-44]. People with preexisting pulmonary and cardiovascular diseases are the most vulnerable group to adverse health effects.

The highest amount of particles exposure may be received indoors, due to the high amount of time spent in these environments. Indoor particles are a mixture of the ambient particles (especially traffic emissions) that easily penetrate buildings and infiltrate indoor air and the particles that are generated indoors during the daily activities (i.e. cooking, smoking...). Therefore higher concentrations of pollutants are reached while these daily activities are done [37-42].

### **1.2.2 Deposition in respiratory system**

One of the risks of UFPs is their high alveolar deposition, due to their small size. They decrease the alveolar capacity to remove foreign particles. Submicron particles are also deposited in the lungs. Particles deposited in the respiratory system are associated with lung cancer induction.

To understand the importance of this effect, a brief description of the respiratory system is explained here. Inhaled particles can be deposited in the lungs or exhaled. Particles are deposited in the lungs with a variable air flow. Between  $10 \text{ m}^3$  and  $25 \text{ m}^3$  of air are processed each day in the respiratory system of an average adult.

The respiratory system can be divided in: head airways region, lung airways or tracheobronchial region and the pulmonary or alveolar region. In this last region is where the gas exchange takes place, hence the importance of UFPs filtration. These regions have different sensitivity to deposited particles among other differences. Some particles are accumulated in each region and do not reach the next one. In the head and lung airways there is the mucociliary escalator, that transports the deposited particles out of the respiratory system in about hours; but the alveolar region does not have this protection. Particles deposited in the alveolar region need a period of months or years to be expelled. Figure 1.1 shows the human respiratory system.

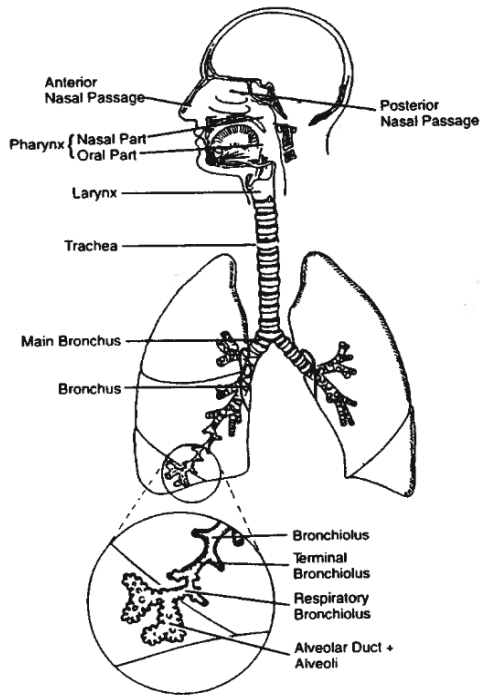


**Figure 1.1: Respiratory system [15]**

The amount and position of particle deposition depends on the size, shape and density of the particle, airway geometry and breathing pattern; it also depends on whether the person breathes through the nose or mouth. Figure 1.2 shows particle deposition in conditions of light exercise and nose breathing. It shows the total deposition and the deposition in the different regions: head airways, tracheobronchial region (TB) and alveolar region (alv).

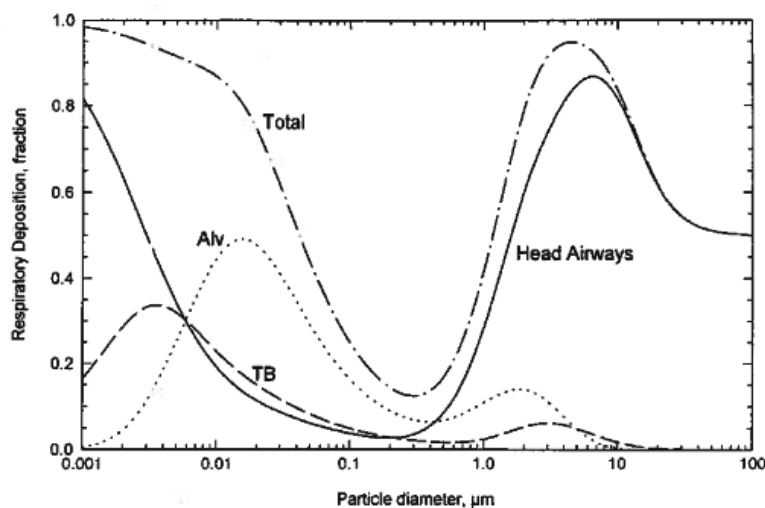


**Figure 1.2: Respiratory deposition [15]**

Figure 1.2 shows that all the regions have high penetration in the UFPs range except for the alveolar region; most of the UFPs bypass the head airways and tracheobronchial region and reach the alveolar region. The figure also shows that the smallest particles, below 0.01  $\mu\text{m}$ , are the ones deposited with higher efficiency in the

tracheobronchial region. Due to the size-selection of the respiratory system, particles larger than 100 nm are not considered dangerous for the alveolar region, while UFPs are. The larger particles, between 2  $\mu\text{m}$  and 10  $\mu\text{m}$ , are deposited with great efficiency in the head airways. Another important conclusion from Figure 1.2 is that submicron particles are the ones with the highest penetration fraction but they are mostly deposited in the lungs. On the other hand, as it is mentioned later in the report, submicron particles are the ones with higher penetration in particle filters.

### **1.2.3 Sick-building syndrome**

Sick-building syndrome (SBS) refers to diffuse symptoms, e.g. reported by workers in modern office buildings. The causes of SBS are not known but one hypothesis is that there is a connection to accumulation of pollutants inside the building when the air-exchange between the building and the outside is inadequate. The SBS symptoms are headache, difficulty concentrating, irritation of the skin and fatigue among others. There is much uncertainty about the exposure that causes these symptoms. The World Health Organization has recognized SBS as a health problem. This health problem is increasing steadily over the years.

The World Health Organization estimates that 30% of the buildings may cause significant health problems to people occupying them. In developed countries, around 60% of all employees work in offices. People suffering SBS have reduced productivity and increased absence from work, which result in significant economic losses. US Environmental Protection Agency estimates that poor IAQ is the reason why 14 minutes of every 8 working hours are wasted and 6 working days for each 10 employees are wasted due to illnesses related to poor IAQ.

Sixty four thousand million dollars are estimated to be lost due to decrease in productivity. To date, no link has been established between UFPs and SBS. However, improving air quality in general may be a way to reduce these symptoms and, therefore, costs.

## **1.3 Purpose and scope of the study**

The purpose of the study is to evaluate UFPs and submicron particles removed by a selection of commonly used filters, available on the market. The present study measures size distributed filtration efficiency and pressure drop of nine different new full-scale filter modules. Two different filter media are tested: glass fiber and charged synthetic. These filters are tested under three air flows, 0.5  $\text{m}^3/\text{s}$ , 0.944  $\text{m}^3/\text{s}$  and 1.3  $\text{m}^3/\text{s}$ ; their corresponding face velocities are, respectively, 1.39 m/s, 2.62 m/s and 3.61 m/s.

UFPs are not considered in the current standards for classification of the studied type of filters; intermediate (fine) filters. This lack of information is an additional motivation.

## **1.4 Outline of the report**

In chapter 2, air filtration is described carefully. In chapter 3 the experimental instruments and the calibration of the test-rig are described. Chapter 4 presents the

experiment results. In chapter 5 the discussions and conclusions are summarized. Finally, chapter 6 shows recommendations for future works. In the end there, is also an appendix with additional information.

## **1.5 Methodology and limitations**

The present study follows an experimental method. First of all, the test-rig was calibrated in order to determine and bound errors in the future measurements. Then different experiments were done to measure the filtration efficiency of different filters.

Due to the time limitation it was not possible to test the filter life time performance. The number of full scale filters tested was also limited. Therefore, the results apply to a selected group of bag filters, commonly used, not only in Sweden, but also internationally. Finally, it is important to note that there could always be an uncertainty in the measurements, even after performing the calibrations.



## 2 Air filtration

Filtration technology is one of the most important methods used for removal of particles. The knowledge of their protection ability against airborne particles, especially the small particles with potentially high risk of health effects, is of crucial importance. In this chapter, filtration theory is introduced and the main air filter types on the market are described.

### 2.1 Filtration efficiency

As mentioned, filtration efficiency defines how well a filter removes airborne particles. From this definition, the filtration efficiency  $E$ , can be calculated:

$$E = 1 - \frac{C_{down}}{C_{up}}$$

where  $C_{down}$  is the average concentration of particles, in particles/cm<sup>3</sup>, at the downstream location and  $C_{up}$  is the average concentration of particles at the upstream location, before the filter.

The particle penetration,  $P$ , of a filter can also be mentioned:

$$P = 1 - E$$

where  $E$  is the filtration efficiency. Penetration defines the fraction of particles that penetrate the filter. This term is also commonly used, but in this project the filters are characterized by their filtration efficiency.

Filtration efficiency depends on filter operation, life time performance and filter material. Some of the factors that affect filtration efficiency are air velocity through the filter medium, particle size, dust loading on the filter, filter packing density, fiber diameter and thickness of the material. Particle penetration is reduced when the filter thickness is increased and when the fiber diameter is decreased.

Air velocity through the filter medium is a function of the filtration area. The velocity of the air through the filter medium,  $v$ , is given by the following expression

$$v = \frac{\dot{Q}}{A}$$

where  $\dot{Q}$  is the volumetric flow rate through the filter and  $A$  is the filtration area.

Figure 2.1 shows filtration efficiency for two different velocities through the filter medium. Generally, collection efficiency increases with decreasing velocity through the filter for particles in the MPPS range.

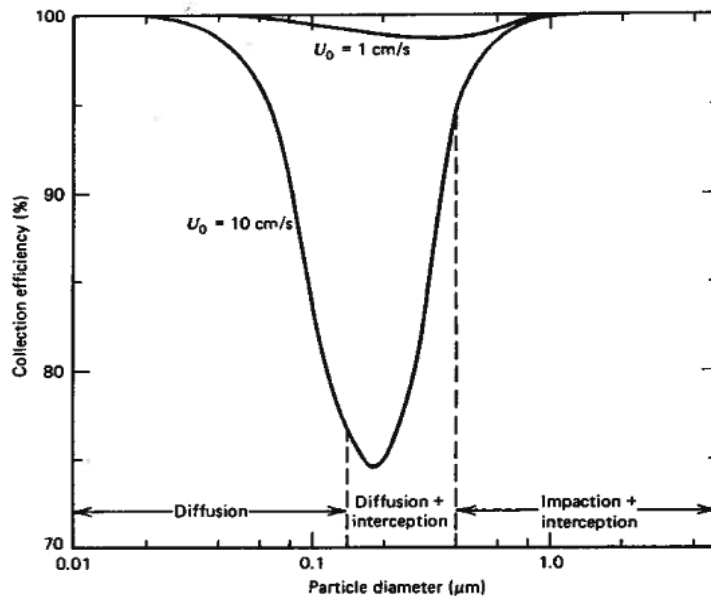


**Figure 2.1: Collection efficiency at two different velocities through the filter medium[15]**

Increasing filtration area gives a better filtration performance because it decreases the velocity through the filter.

## 2.2 Criteria of filter selection

### 2.2.1 Filter class in standards

The European Standard EN 779 and the American Standard ASHRAE 52.1 and 52.2 are used for classification of coarse and intermediate ventilation air filters. The classification of these filters was made based on the collection efficiencies obtained in several experiments.

The American Society of Heating, Refrigerating and Air-Conditioning Engineers (ASHRAE) has established in its standards the terms dust spot efficiency and minimum efficiency reporting value (MERV) for manufacturers to assess filter's performance. To measure the efficiency, twelve size ranges of particles are used. The smallest particle size considered is 300 nm.

Coarse dust filters and fine dust filters are frequently used in air filtration. Based on their collection efficiency, standard EN 779 classifies the different fine filters into five classes, F5, F6, F7, F8 and F9 where F5 is the less efficient and F9 the most efficient. The filter classes are G1, G2, G3 and G4 for coarse dust filters. The classification is done based on the average filtration efficiency with respect to liquid DEHS particles of 400 nm.

In this project, nine different intermediate (fine) filters have been tested. The tested filters belong to filter classes F5-F9, according to the European standard EN779. One of the air flows tested in the experiments,  $0.944 \text{ m}^3/\text{s}$ , is the standard air flow in EN 779.

The choice of a filter depends on many factors, such as the type and size of particles that the filter is supposed to remove. In most cases it is not possible to remove all the airborne pollutants. Particles that must be removed can vary depending on where the filter is located; for example, the filtration requirements are different in a hospital than in a kitchen or a factory. Special importance should be paid in ventilation of hospital facilities. Once the filtration efficiency is selected, other factors should be considered, like resistance to air flow (directly proportional to energy consumption) in order to reduce filtration costs.

If the only goal was filtration efficiency, then a High Efficiency Particulate Air (HEPA) filter would be used. This unit provides the higher efficiency but the energy costs are so high that it is not a real possibility in most cases.

Filters with higher efficiency usually are the ones with higher pressure drop. A filter with a very high efficiency may not be recommended because of the high energy consumption required. The ideal filter is the one that provides the highest efficiency with the least pressure drop. F5-F9 filters are commonly used in Europe. Filters of class F7 are commonly used to filter the supply air in commercial buildings.

### 2.2.2 Pressure drop

Pressure drop is an important commercial criterion of filter selection. Pressure drop in a fibrous filter is the resistance to the air flow across the filter caused by the effect of each fiber resisting the air flow; it represents the total drag force of all the fibers. The pressure drop is calculated with the following expression:

$$\Delta p = \frac{\eta t U_0 f(\alpha)}{d_f^2}$$

$$\alpha = \frac{\text{fiber volume}}{\text{total volume}}$$

where  $\eta$  is the dynamic viscosity,  $t$  is the filter thickness,  $U_0$  is the face velocity,  $\alpha$  is the packing density,  $f(\alpha)$  is a function of the packing density and  $d_f$  is the diameter of the fibers.

Ideally, the pressure drop is directly proportional to the flow rate; inside most filters the air flow is laminar, and it depends on the filter media and on the filter housing. However, typically a turbulent component makes the pressure drop proportional to the air flow rate to the power of an exponent slightly above 1 (one).

The ability of an air handling unit, AHU, to move air through the system is reduced when the pressure drop increases. When this ability is reduced, more energy is required to provide the same air flow. When the efficiency of a filter increases, the pressure drop usually increases too.

## 2.3 Filters

Filtration of aerosol particles is a common method for particle removal. An aerosol is a suspension of fine solid particles or liquid droplets in a gas. The different kinds of filters used in this project are described below.

### 2.3.1 Fibrous filters

Fibrous filters are particle filters formed by a mat of fine fibers that are mostly perpendicular to the direction of the air flow. The level of porosity is high in this kind of filters. Fibrous filtration is a complex process due to neighboring fiber interference effect and the deviation from the ideal flow patterns due to the random orientation and inhomogeneity of the fibers.

The ability of these filters to collect particles depends on particle size, shape, charge and other factors. The most common fibrous filters are cellulose fibers, glass fibers and plastic fibers.

In the experiments, three different fibrous filters were used: filters made from uncharged fiberglass (glass fiber filters) and two kinds of plastic fiber filters, which are charged synthetic filters and a nano-fiber filter.

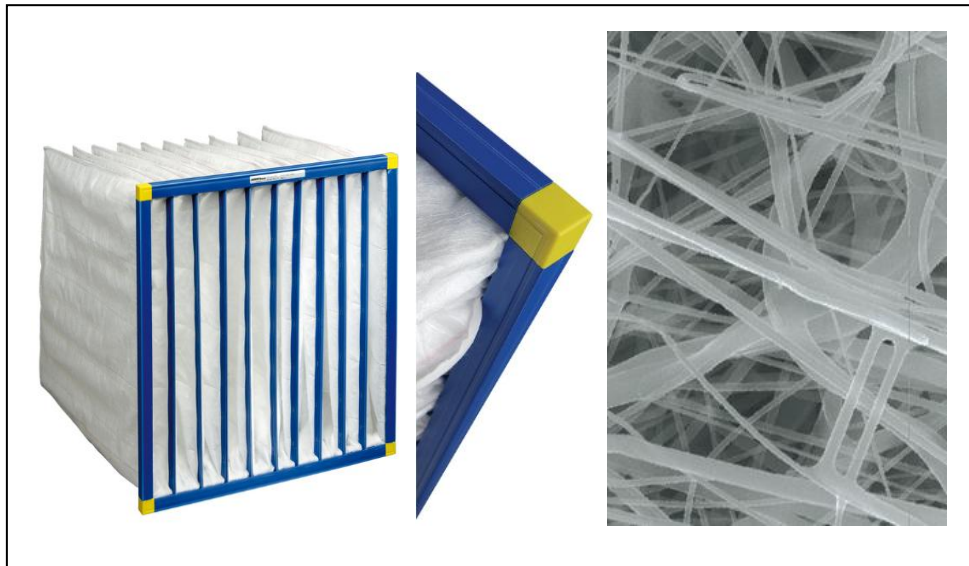
Glass Fiber (GF) filters are made of glass fiber. The fibers of this kind of filter are not electrostatically charged. Glass fiber filters media is quite complicated. They are made from a combination of different filter layers that contribute to filtration performance.

Figure 2.2 shows a glass fiber filter of 8 bags.



**Figure 2.2: Glass Fiber filter**

Charged synthetic (CS) filters are made from electrostatically charged fibers. They create electrostatic fields which enhance collection of electrically charged particles. Electrostatic forces can be much greater than the gravitational or inertial forces. Figure 2.3 shows one charged synthetic filter, which has 10 bags. The fibers of this kind of filter and the level of porosity can be clearly seen in the illustration.



**Figure 2.3: Charged Synthetic filter**

Nano-fiber filters are filters made of fibers with a size smaller than  $1\mu\text{m}$ . In the experiments, a filter with a mix of about 10% of nano-fiber is tested. If the number of nano-fibers was higher, then the pressure drop would be greatly increased; this is the reason why this kind of fibers represents no more than 10% in these filters. Nano-fiber filters are supposed to enhance collection efficiency. In this study, it is assumed that the nano-fiber filter is made of charged fibers, as there is no available data about its material.

Well-designed synthetic filters are expected to operate with a pressure drop noticeably lower than glass fiber filters with the same efficiency.

As shown in Figure 2.1, the efficiency curves are U shaped. The observed MPPS range is expected to be approximately 110-200 nm for glass fiber filters [8,15,27], while the MPPS for electrostatic filter media is estimated to be around 30-60 nm [14]. This minimum efficiency corresponds to submicron particles and, in charged synthetic filters, to UFPs.

The inverse relationship between air velocity through the filter medium and filtration area has been mentioned. To achieve higher efficiencies, filters have some bags or have a pleated filter medium in order to increase the filtration area. The filters tested in the experiments have several bags, as shown in Figures 2.2 and 2.3. There are other advantages of increasing filtration area, such as the increased lifetime of the filter due to the increased dust holding capacity, the reduced pressure drop or the decrease in noise generation (due to the fan operating at a lower pressure rise).

### **2.3.2 High Efficiency Particulate Air filter**

The experiments on the filtration efficiency have been carried out using a so called HEPA filter for pre-filtration. A traditional definition of HEPA filters is that they remove particles of 300 nm with an efficiency of 99.97% or higher. However, according to the European standard for classification of HEPA filters (EN 1822) these filters are classified with respect to removal of MPPS-sized particles - which

generally are smaller than 300 nm. The EN 1822 standard also comprises the so called ULPA-filters (Ultra Low Penetration Air). ULPA-filters are of the same type as HEPA-filters, but they have even higher efficiencies.

HEPA- and ULPA-filters are of vital importance in some significant applications, where an extremely high particle collection is required. They are used in nuclear facilities and biological safety cabinets, among others applications.

HEPA filters provide greater protection from airborne particles than the intermediate filters studied in this thesis; their application is greatly limited by its extremely high pressure drop under high air flow rates.

One example of a HEPA filter construction is based on a fibrous mat made of fine glass fibers with a support layer of cellulose. In order to increase the filter area, this fiberglass paper is pleated.

During the experiments, a HEPA filter of class H14 according to EN 1822 has been used as a pre-filter upstream of the tested intermediate filter. Figure 2.4 shows the HEPA filter used.



**Figure 2.4: HEPA filter**

## **2.4 Problems of filter application**

Particle filters characteristics change with dust loading. Different problems faced when using air filters are discussed here. The major problems in filters' life cycle are summarized here.

### **2.4.1 Increase of pressure drop**

The pressure drop increases with time because the resistance to the air flow is increased with the particles captured in the filter. As the resistance to the air flow increases, more energy is required to maintain the same air flow rate. However, if the fan capacity is not controlled, the airflow rate will decrease as the pressure drop increases.

## **2.4.2 By-products from used filters**

For traditional filters, particulate pollutants are caught and remain there until the filter is cleaned or changed. Additionally, in Europe, ventilation air filters are frequently replaced after 0.5-1 year of operation.

It is important to notice that, under the influence of moisture, some microorganisms can grow from deposited organic material and lead to unpleasant odors. These unpleasant odors may annoy people occupying indoor spaces and are a source of SBS.

When employing used filters there is also a risk that pollutants from the air accumulated in the filter will be released. At some point the pressure drop may be excessive, because of the dust accumulation, and the filter will be clogged. In this case, the filter may release some of the accumulated dust agglomerates. If this happens, the air after the filter may be more polluted by the used filter.

## **2.4.3 Reduced efficiency of charged synthetic filters**

Glass fiber filters and charged synthetic filters have different performance when the filter has dust accumulated.

In glass fiber filters, the fiber diameters are important to filtration efficiency; typically, the efficiency increases in used filters because of the particles accumulated in the filter. In this kind of filters, usually the initial efficiency is the minimum efficiency and it increases with time. Most of the available data show that the efficiency of used filters is higher than for the new ones.

On the other hand, the efficiency for charged synthetic filters may decline with time. The charges on the fibers are shielded because of collected dust particles, and the filtration efficiency is considerably lower than for the clean filters.

## **2.4.4 Bypass of air flow**

The frame of a filter holds the filter inside the ventilation duct. Filter bypass is the amount of air that does not go through the filter because of the existence of gaps between the frame and the duct. It depends on the size and geometry of the gaps around the filter and also on the pressure drop and efficiency of the filter.

The air flow through the system would split into two different flows: one passing through the filter medium and the other one bypassing the filter. Depending on the size of the gap, the effects on the performance of the filters are different. If the gap is around 1 mm the performance of the filter is not significantly affected. The larger the gap is, and hence the higher the bypass flow, the more influence it has on filter performance and the larger the error when calculating the efficiency. A gap around 10 mm can make the filtration efficiency reduce 30%. Even moderate gaps can dramatically affect filtration efficiency [13].

Bypass effect is increased with higher pressure drops. The more efficient filters are usually the ones with higher pressure drop and, therefore, they are also the most sensitive to air bypass. This means that not always a more efficient filter has a better performance; if an efficient filter has a high air bypass, its performance could be

reduced to one characteristic of a lower filter class. The lowest pressure drop is reached in new filters, before the dust is accumulated; bypass flow increases during the lifetime of a filter.

It was mentioned before that the efficiency of glass fiber filters usually increases with dust accumulation. However, if air bypass is considered, this conclusion can change when there is an important gap between the duct and the filter frame.

## 2.5 Deposition mechanisms

Fibrous filters remove particles when they collide and attach to the surface of the fibers.

Particulate air filters capture particles in different ways. When the opening between fibers is smaller than a particle, the particle cannot pass through. Most of the time the particles are smaller than this gap and this method is not effective. The overall filtration efficiency can be calculated from the single fiber efficiency, which is the efficiency of each fiber. Single fiber efficiency can be estimated as the sum of the single fiber efficiency for each one of the different deposition mechanisms.

$$E = 1 - (1 - E_I)(1 - E_R)(1 - E_D)(1 - E_G)(1 - E_{DR})$$

$$E \approx E_I + E_R + E_D + E_G + E_{DR}$$

Below there is a brief description of the five deposition mechanisms. All except electrostatic attraction are mechanical collection mechanisms.

- Inertial impaction: is the most important filtration mechanism for large particles. High density large particles have great inertia that makes them reluctant to changes in air flow direction. As the streamlines change near the filter's fibers, these particles hit the fiber and remain there. The single fiber efficiency associated to this mechanism is  $E_I$  and increases with particle inertia, air velocity and with a more abrupt curvature of streamlines.

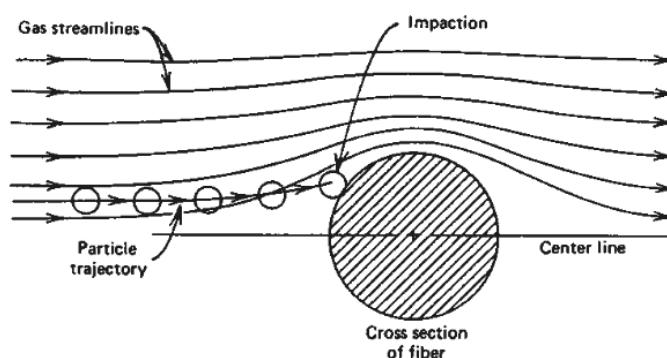
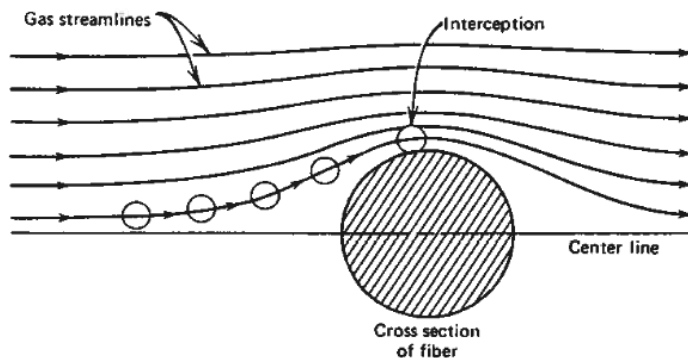


Figure 2.5: Inertial impaction [15]

- Interception: is also important for large particles and in the MPPS range. This mechanism occurs when one particle, which follows an air streamline, hits the fiber and is trapped. This happens when the distance between the fiber and the streamline is within the particle radius. This mechanism is enhanced when the fiber and the particle have comparable sizes and is the only mechanism that does not depend on  $U_0$ . For a given particle size not all the streamlines will end in the collection of the particle. The single-fiber efficiency for interception is represented by  $E_R$ .



**Figure 2.6: Interception [15]**

- Diffusion: very small particles collide with a filter-media fiber and remain attached by van de Waals force; because of their Brownian motion, these small particles can hit the fiber when their streamline is not intercepted by the fiber. Particle diffusion increases with smaller particles and is of special importance for particle diameters below  $0.1\mu\text{m}$ .  $E_D$  is the single-fiber efficiency for diffusion and is decreased with increasing air velocity.

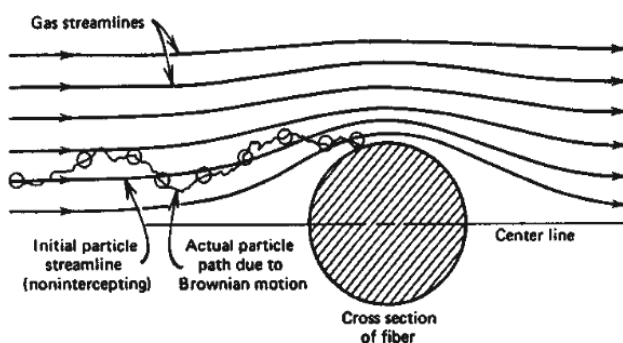


**Figure 2.7: Diffusion [15]**

- Gravitational settling: this mechanism has a smaller efficiency than the others, except when the particle size is large and the face velocity is low. If the air flow is against gravitation then gravitational deposition

is negative, i.e. it decreases single-fiber filtration efficiency. This efficiency is represented as  $E_G$ .

- Electrostatic attraction: to quantify electrostatic deposition is necessary to know the charge on the particles and on the fibers because the efficiency increases with the charge. The efficiency is also increased with decreasing face velocity. When there is no significant charge in the particles or in the fibers, this mechanism is neglected but when these charges appear, the mechanism is highly important. When a fiber is charged, it induces an electric field, creating a force in the direction of the fiber and forcing the particle to follow that direction. When the charge is on the particles, coulombic attraction enhances collection. Charged fibers have a positive impact in filtration efficiency without increasing the pressure drop. In the other hand, this charge can be lost when working with ionizing radiation or organic liquid aerosols, high humidity or temperature and when dust is accumulated.

It is important to consider the effect of the enhance collection efficiency in the range of the MPPS due to interception of the diffusing particles. This interaction is considered in the overall efficiency as  $E_{DR}$ .

Figure 2.8 shows the contribution of each mechanism for each particle size for some specific conditions, like  $V=0.10$  m/s.

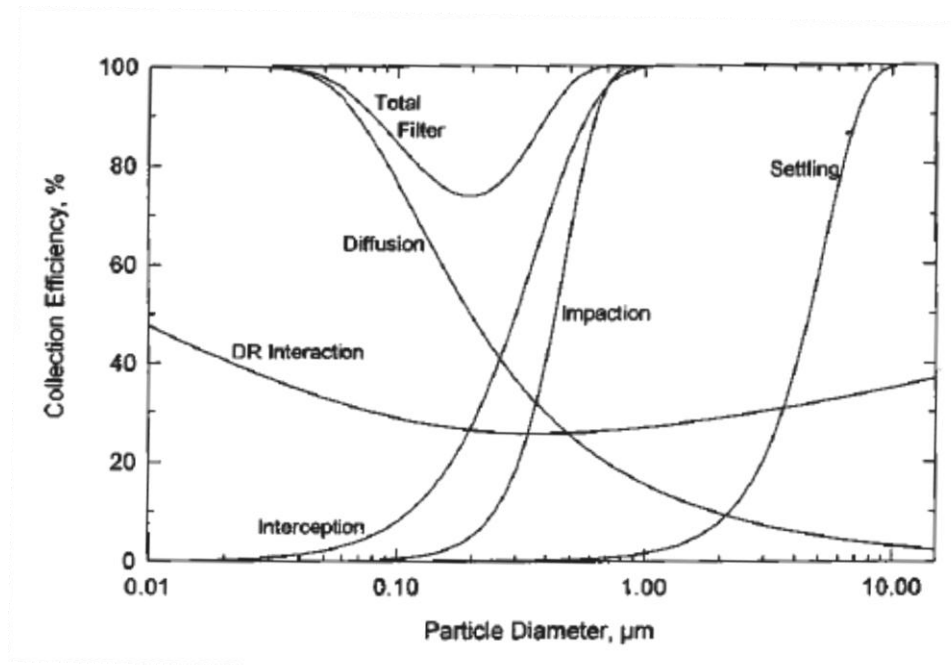


**Figure 2.8: Collection efficiency [15]**

The figure highlights the almost irrelevant contribution of gravitational settling for the smaller sizes. The deposition rates and, therefore the efficiency, are higher for the

smallest particles and for the biggest particles because diffusion and gravitational settling are large on them, respectively. This is the reason why filtration efficiency curves are U-shaped.

## 2.6 Power consumption

To overcome the pressure drop, power consumption is necessary. This power, called air power  $W$ , is calculated as follows:

$$W = \dot{Q} \times \Delta p$$

where  $\dot{Q}$  is the air flow rate and  $\Delta p$  is the pressure drop.

The electrical power,  $W_e$ , is given by:

$$W_e = \frac{W}{\eta_m \eta_T}$$

where  $\eta_m$  is the motor efficiency and  $\eta_T$  is the fan total efficiency.

The power consumption is increased when the area of the fibrous filter is decreased; this is because of the increase in pressure drop. To estimate the energy use it is important to know the average pressure drop.

## 2.7 Costs

Although the demand for a better IAQ is growing, the requirements for a reduction in costs are also enhanced. Air filtration reduces energy costs; it reduces the need of cleaning both the occupied space and the HVAC ducts. Air filtration also reduces health risks of occupants, which gives the additional benefit of a reduction of the productivity loss.

Nowadays it is common to replace filters yearly. Air filtration costs include both initial and annual running costs. The initial costs or investment costs include the cost of the filter, racks and fans. The annual running costs include the power consumption to move the air through the filters and the maintenance and disposal of filters. Disposal is a significant part due to the importance of recycling, but the highest contribution to annual costs is the energy consumption.

The energy cost of a filter can be calculated with the following expression:

$$C = W_e \times h \times e$$

where  $h$  is the operating hours and  $e$  is the price of electricity.

As mentioned before, the higher the air flow and pressure drop, the higher the fan power, which means the higher the energy cost. Replacing filters with other ones with a lower average pressure drop can save energy. A sooner replacement of filters could

save energy and, hence reduce costs. Due to the influence of the pressure drop on energy consumption, more efficient filters usually have a higher cost.

The cost per unit air flow is estimated with the expression:

$$\text{Cost per unit airflow} = \frac{\text{Filter cost} + \text{Labor cost per filter installation} + \text{Energy Cost}}{\text{Filter lifetime} \times \text{Airflow rate}}$$

$$\text{Filter lifetime} = \frac{\text{Dust Holding Capacity}}{\text{Arrestance} \times \text{Inlet Particle Concentration} \times \text{Airflow Rate}}$$

It should be noted that prediction of filter lifetime is complicated in practice. This has to do with the standard test dust used to “load” the filter (to obtain an increase of the pressure drop). Standard tests rarely or never reflect the real dust holding capacity or pressure drop increase.

### 3 Tests planning

A schematic diagram of the experimental set-up is shown in Figure 3.1.

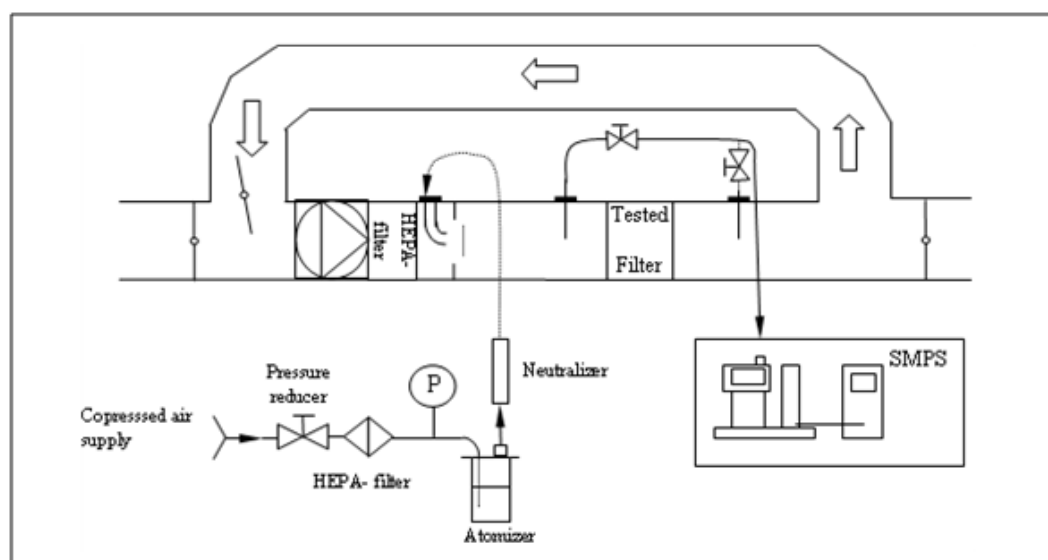


**Figure 3.1: Experimental set-up**

The test-rig was operated as a closed system with a fan and a HEPA filter. Tested filter shows the place where the filter is inserted. The arrows show the direction of the air flow; the experiments are done in a recirculated system. The atomizer aerosol generator injects the aerosol after the HEPA filter. This ensures that the air is clean before the aerosol is injected and, therefore, all the particles inside the system are the ones generated with the atomizer. In some of the experiments, the aerosol passes through a neutralizer before injected inside the test-rig. The Scanning Mobility Particle Sizer (SMPS) spectrometer measures the particle concentration up and downstream of the tested filter, as shown in the figure. The manometer is not in the figure, but the pressure drop measurements are taken just after and before the tested filter. This makes it possible to measure the pressure drop induced by the filter.

Single pass efficiency is measured in the experiments; it is a quick method and isolates the filter. On the other hand, the duct system is ignored but, as the study is focused on the filters, this does not represent a disadvantage.

The aerosol injected in the test-rig is generated by a TOPAS atomizer ATM 230 and then passes/does not pass the neutralizer. Two different aerosols are injected in order to compare the influence of the challenge aerosol in the experiments.

### 3.1 Experimental instruments

#### 3.1.1 Ultrafine particle counter

TSI P-Trak, model 8525, ultrafine particle counter was used for the calibration of the test-rig. P-Trak is a portable condensation particle counter which can detect the total particle number concentration in the size range between 20 nm and 1000 nm. It is

based on TSI industry condensation particle counting technology and gives real-time results. In the experiments, the instrument records the average particle concentration in 10 seconds. P-Trak gives particle concentrations in particles per cubic centimeter (particles/cm<sup>3</sup>).

The main specifications of the P-Trak are summarized in table 3.1.

**Table 3.2: P-Trak specifications**

Concentration range	0 to $5 \cdot 10^5$ particles/cm <sup>3</sup>
Particle Size Range	0.02 to greater than 1 $\mu\text{m}$
Temperature range in operation	0 to 38°C

Figure 3.2 shows the P-Trak that has been used in the tests.



**Figure 3.1: P-Trak**

### 3.1.2 Air velocity and pressure differential measurements

An instrument of model Swema air 300 was used with two different sensors: SWA 31 and SWA 10, that measured air velocity and pressure drop, respectively. This instrument was used to calibrate the test-rig and to measure the pressure drop for the different filters and the overpressure inside the duct.

Swema air 300 is shown in Figure 3.3.



**Figure 3.3: Swema air 300**

### 3.1.3 Atomizer aerosol generator

An atomizer aerosol generator, model ATM 230 from TOPAS, was applied in the experiments. This instrument produces test aerosols with known properties, highly stable particle size distribution and high reproducibility of the particle concentration. Different aerosol substances may be used, e.g. DEHS and PAO, and it is also suitable for salt aerosol production. The highest concentration of particles generated is mainly in the range of 100-300 nm, close to the MPPS. The amount of particles generated in this range is higher than  $10^7$  particles/cm<sup>3</sup>.

Two types of aerosols were generated in the experiments: DEHS oil and NaCl.

The schematic diagram in Figure 3.4 shows the intake of air of the aerosol generator. The internal HEPA filter is located there to remove ambient particles from the air. This ensures that the compressed air is clean and therefore all the particles in the air injected inside the test-rig are the ones generated by the aerosol generator.

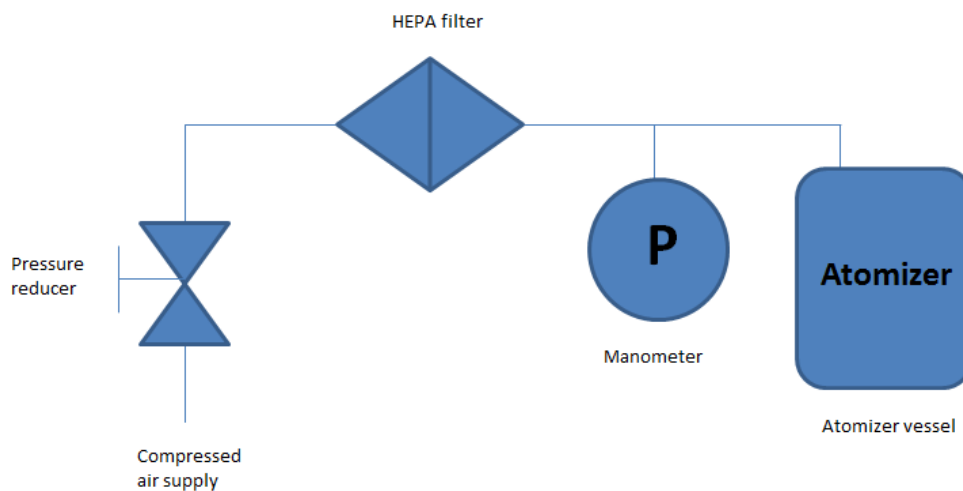


**Figure 3.4: Aerosol generator diagram**

Relevant specifications are shown in Table 3.3.

**Table 3.3: Aerosol generator specifications**

Flow rate	500-2500 l/h
Particle number concentration (DEHS)	$>10^8$ particles/cm <sup>3</sup>
Particle size (mode value DEHS)	0.2-0.3 $\mu$ m
Mass flow rate	max. 20 g/h
Continuous operating time (0.5 l)	approx. 16 h
Atomizer pressure	1.5-6 bar
Dimensions	230x380x225 mm

Figure 3.5 shows the aerosol generator.

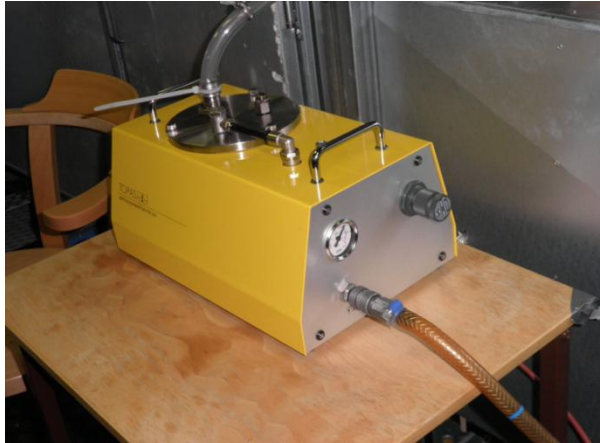


**Figure 3.5: Aerosol generator**

Tables 3.4 and 3.5 show some physical data of DEHS and NaCl, respectively.

**Table 3.4: DEHS physical data**

Name	Di ethyl hexyl sebacate
Formula	$C_{26}H_{50}O_4$
Molar mass	426.69 g/mol
Density	$0.912 \text{ g/cm}^3$

**Table 3.5: NaCl physical data**

Name	Sodium chloride
Formula	NaCl
Molar mass	58.45 g/mol
Density	$2.2 \text{ g/cm}^3$

### 3.1.4 Scanning Mobility Particle Sizer spectrometer

To measure the particle concentration, a Scanning Mobility Particle Sizer (SMPS) spectrometer, offered by TSI, has been used. One of the many applications of the SMPS is to test filter efficiency; most studies on UFPs use this technology in their research. This kind of spectrometers uses electrical-mobility particle size classification and a Condensation Particle Counter (CPC).

SMPS Series 3936 is the one used in the lab. The series 3936 SMPS spectrometers, feature TSI Series 3080 Electrostatic Classifiers, consist of a Differential Mobility Analyzer (DMA) and a Condensation Particle Counter (CPC).

Figure 3.6 shows the different components of series 3936:

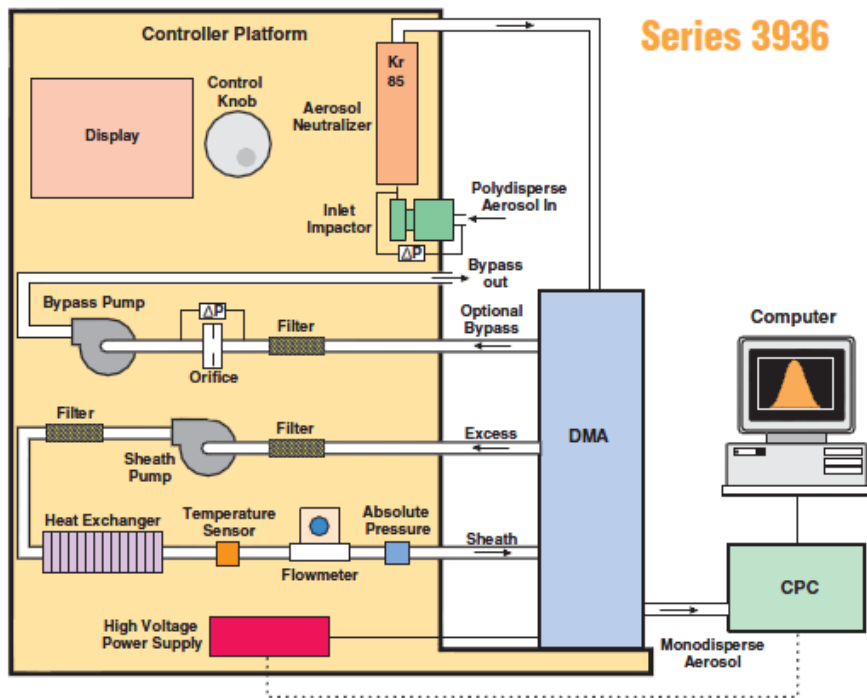


**Figure 3.6: SMPS components**

The operation is as follows: First, the aerosol sample passes through an inertial impactor that removes large particles outside the measurement range in order to minimize errors. Then, the aerosol passes through a bipolar ion neutralizer that charges a large fraction of the particles passing the neutralizer. After that, all aerosol particles, neutral and charged, enter a DMA which separates particles corresponding to their electrical mobility. Negatively charged particles are repelled and deposited on the outer wall, neutral particles exit the DMA with the excess air and positively charged particles move towards the negative inner electrode. Finally, only some particles with a narrow range of electrical mobility can leave the DMA and reach the CPC that, at last, measures with high precision the particle concentration.

Characteristics of SMPS spectrometer used are shown in the following table:

**Table 3.6: SMPS specifications**

Particle size range	4 nm to 1000 nm
Particle concentration	2 to $10^8$ (particles/cm <sup>3</sup> )
Measurement time	30 to 600 sec (selectable)
Channels per decade	16
Key feature	Highest-resolution; individual components provide greatest flexibility
DMA	3081
CPC	3775
Condensing liquid	n-butyl alcohol

Figure 3.7 shows the SMPS used in the lab.



**Figure 3.7: SMPS**

### 3.1.5 Neutralizer

The aerosol particles generated are usually electrostatically charged. Generally a high level of electrical charge increases particle loss in the system and may affect the efficiency obtained in the experiments. The neutralizer ionizes the atmosphere because of the action of a radioactive source (Kr-85 or Po-210). Aerosol charged particles are discharged because they capture ions of the opposite charge, reaching equilibrium.

Some of the experiments have been done using the neutralizer model 3012A from TSI.

Important specifications of the aerosol neutralizer are summarized in table 3.6 and Figure 3.8 shows the instrument.

**Table 3.7: Neutralizer specifications**

Source	Kr-85
Emission	Beta decay
Radioactivity	370 MBq
Half life	10.7 years
Maximum flow rate	50 l/min
Maximum temperature	50°C
Maximum pressure	35 kPa
Outer housing material	Anodized aluminium
Inlet diameter	1.27 cm
Outlet diameter	1.27 cm
Housing diameter	7.72 cm
Overall length	52.86 cm
Weight	1.0 kg

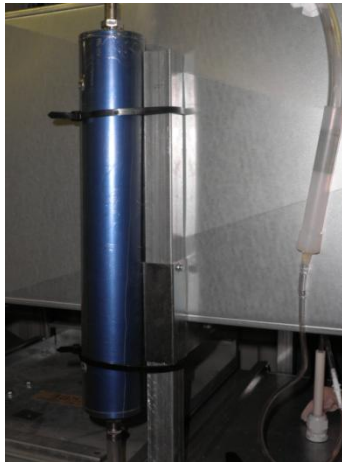


**Figure 3.8: Neutralizer**

Figure 3.9 shows how, after leaving the aerosol generator, the aerosol passes through the neutralizer and then is injected inside the test-rig.



**Figure 3.9: Aerosol generator and neutralizer**

Although it is mentioned later in the report, it is important to highlight that in the experiments with DEHS aerosol, the aerosol generator probably supplies uncharged particles, and the interaction with the neutralizer will charge them slightly.

## **3.2 Qualification of test-rig**

All the experiments have been done in a test-rig from Chalmers University of Technology. Figure 3.10 shows this test-rig.



**Figure 3.10: Test-rig**

The main specifications of the test-rig are shown in table 3.8.

**Table 3.8: Test-rig specifications**

Air flow rate	250-1000 l/s
Air velocity	0.69-2.78 m/s
Temperature	20-24°C
Humidity ratio	20-80%
Cross section area	0.6*0.6 m <sup>2</sup>

The calibration of the test-rig informs whether the results obtained from the experiments are accurate or not.

The background concentration is the concentration of particles inside the test-rig when there is no aerosol injected. This concentration was measured and it is negligible, hence it is not considered in the calculations.

For the present study major parts of the Swedish and also European standard SS-EN 779 have been followed; this European Standard deals with the performance testing of particulate air filters for general ventilation. This section describes the different tests recommended by the standard.

### **3.2.1 Uniformity of the air velocity**

The purpose of this test is to prove that the air velocity is uniform over the test-rig cross-section. This ensures that both upstream and downstream measurements are done at the same air flow.

Air velocity is measured on nine different points, in both upstream and downstream sections, in order to determine the uniformity of the air velocity in the test duct. The layout of the measurements is depicted in Figure 3.11.

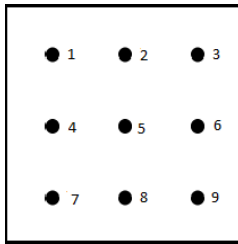


**Figure 3.11: Sampling points for air velocity uniformity and aerosol uniformity**

The Swema SWA 31 probe was used to measure the air velocity. Three measurements have been taken for each point in order to use the average to calculate their standard deviation,  $\delta$ . With this information the coefficient of variation, CV can be easily determined:

$$CV = \frac{\delta}{\mu}$$

where  $\delta$  is the standard deviation and  $\mu$  is the mean value of the air velocity measured in the nine points.

The standards require a CV lower than 10% to prove that the air velocity is uniform.

This test has been done for three different air flow rates: 0.25 m<sup>3</sup>/s, 1.0 m<sup>3</sup>/s and 1.5 m<sup>3</sup>/s. The resulting data can be found in Table 8.1-8.6 in the appendix. As shown in the tables, CV<10% at each air flow, which means that the air velocity is uniform.

### 3.2.2 Aerosol uniformity in the test-rig

It is important that the aerosol concentration is the same all over each section. When the aerosol is injected inside the test-rig, the inserted tube is divided into four exits, in order to distribute the aerosol.

The challenged aerosol uniformity is also analyzed at 9 points and three different air flows in the test-rig, in the upstream sampling section, immediately before the filter. The P-Trak is used in this case. As in the previous test, different values for each point are taken, and, as for the air velocity uniformity test, the coefficient of variation is calculated. To prove the uniformity this coefficient must be less than 15%. The results of this test are shown in the appendix, in Tables 8.7, 8.8 and 8.9.

### 3.2.3 Particle counter zero test

The air must be clean after passing the HEPA filter. The particle concentration was measured with the P-Trak in three different points in the upstream section, before the place for the filters, and the result was successful.

### 3.2.4 Particle counter overload test

This test was conducted to prove that the concentration in the duct is never higher than the concentration limit CL of the SMPS used. In this case, this CL is 10<sup>8</sup> and the

highest concentrations reached are never higher than this value. If the concentrations reached were above the limit, the SMPS would not be able to read them accurately.

The highest concentration of particles is reached for the minimum air flow. In the appendix, in Figure 8.1 a graph with the concentration of particles for  $0.5 \text{ m}^3/\text{s}$  is shown to prove that this concentration is always lower than  $10^8$ .

### **3.2.5 100% efficiency test**

The aim of this test is to make sure that a 100% efficiency measurements are provided by the test duct and sampling systems.

Due to filter mount limitation, the HEPA filter cannot be mounted at the test location. That is the reason why the HEPA filter is placed upstream and it is tested that the test-rig can provide clean air: above 99% efficiency for all particle sizes.

### **3.2.6 Zero % efficiency test**

The zero % efficiency test is done to prove the precision of the duct, sampling system, measurement and aerosol generation systems.

Without any filter inside the duct, the concentration of particles up and downstream was measured with the P-Trak; the efficiency obtained must be smaller than  $0\% \pm 7\%$ . The results of this test proved that the efficiency is, in all the cases, smaller than  $0\% \pm 2\%$ ; the results are shown in the appendix, in Table 8.10.

### **3.2.7 Aerosol generator stability**

The aim of this test is to demonstrate that the aerosol concentration does not change inside the test-rig when there is no filter inside.

The concentration of particles was measured upstream and downstream in the test-rig, without using any filter, when using the aerosol generator. These measurements were done with the SMPS and the results showed that the aerosol generated was stable. Figure 8.2 in the appendix show the generated DEHS aerosol in the upstream location. With the atomizer working at 4 bar and an air flow in the test-rig of  $0.944 \text{ m}^3/\text{s}$ , the measurements were taken. The average and standard deviation are obtained from continuous measurements during 35 minutes.

### **3.2.8 Over-pressure checking**

The purpose of the over-pressure checking between the inside and the outside of the test-rig is to ascertain that, after the HEPA filter, the duct has always over-pressure in relation to the outside of the test-rig. This indicates that there is no important leakage into the test-rig that may affect the particle concentration.

The measurements have been done in 3 sections: just before (section 1) and after the place where the tested filter is placed (section 2), and in the section where the downstream measurements are done (section 3). No filter was used for this test. For the first and the third measurement sections, three different measurement points were

used; for the second section, only one. This test was done for two different air flows:  $0.25 \text{ m}^3/\text{s}$  and  $1.5 \text{ m}^3/\text{s}$ .

In the appendix, Tables 8.11 and 8.12, show the static pressure differences between the inside and the outside of the test-rig. The observed overpressure of 0-15 Pa indicates that leakage of particles into the test-rig can be neglected.



## 4 Experimental results

While performing the calibration of the test-rig it was checked that there was almost no background concentration of particles, hence this concentration is neglected in all the calculations. Once the calibration of the test-rig is done, the experimental work can start. In the following sections, the results of the diverse experiments are shown.

Table 4.1 presents the different filters tested in this thesis.

**Table 4.1: Filters tested**

Filter Sample	Filter class		Filter media type	Filter size
	European standard EN 779	US standard ANSI/ASHRAE 52.2		
#1	F5	MERV 9-10	Charged Synthetic	592*592*500_4 bags
#2	F6	MERV 11-12	Charged Synthetic	592*592*635_8 bags
#3	F6	MERV 11-12	Glass Fiber	592*592*500_10 bags
#4	F7	MERV 13	Charged Synthetic	592*592*635_8bags
#5	F7	MERV 13	Glass Fiber	592*592*500_10 bags
#6	F7	MERV 13	Nano-fiber	592*592*635_8 bags
#7	F8	MERV 14	Charged Synthetic	592*592*635_8 bags
#8	F8	MERV 14	Glass Fiber	592*592*450_8 bags
#9	F9	MERV 15	Charged Synthetic	592*592*635_8 bags

Most of the experiments were done at three different air flows: 0.5 m<sup>3</sup>/s, 0.944 m<sup>3</sup>/s and 1.3 m<sup>3</sup>/s. As shown in the table, not all the filters have the same surface area. Filters #1 and #8 have a different filter area. In order to obtain the same air velocity through the filter medium as for the other filters, the air flow rate used for some tests is different.

The face velocity,  $U_0$ , is the velocity of the air just before it enters in the filter and can be calculated as follows:

$$U_0 = \frac{\dot{Q}}{A}$$

where  $\dot{Q}$  is the air flow (m<sup>3</sup>/s) and  $A$  (m<sup>2</sup>) is the cross-sectional area of the filter exposed to the airstream. Once inside the filter, the face velocity is increased slightly due to the reduction of the volume. This velocity is calculated like:

$$U = \frac{\dot{Q}}{A(1-\alpha)}$$

where  $\alpha$  is the packing density.

As the difference is very small, this variation in the face velocity is not considered.

The following expression shows how to calculate the total area for the filters:

$$A = 2 \times Nbags \times (H \times L)$$

where  $Nbags$  is the number of bags of the filter,  $H$  is the height of the filter frame and  $L$  is the length of the bags.

In order to calculate the air velocity through the filter medium,  $V$ , the total area above is used.

Using this expression for filters #2, #3, #4, #5, #6, #7 and #9, the air flow and the air velocity through the filter medium are  $\dot{Q}=0.5 \text{ m}^3/\text{s}$ ,  $0.944 \text{ m}^3/\text{s}$  and  $1.3 \text{ m}^3/\text{s}$ ; and  $V=0.084 \text{ m/s}$ ,  $0.159 \text{ m/s}$  and  $0.219 \text{ m/s}$ , respectively.

The tested air flows give face velocities of  $U_0=1.39 \text{ m/s}$ ,  $2.62 \text{ m/s}$  and  $3.61 \text{ m/s}$ , respectively.

Filter #1 (F5 charged synthetic) has been tested with air flows equal to  $0.5 \text{ m}^3/\text{s}$ ,  $0.944 \text{ m}^3/\text{s}$  and  $1.3 \text{ m}^3/\text{s}$ . The reason why these air flows have been chosen is explained by the fact that F5 filters with a different area are not normally found. Although F5 filter area is different they usually do not have a high number of bags. These air flows give different velocities through the filter medium, which are, respectively,  $V=0.211 \text{ m/s}$ ,  $0.398 \text{ m/s}$  and  $0.549 \text{ m/s}$ .

The air flows that have been used for filter #8 (F8 glass fiber) are  $\dot{Q}=0.358 \text{ m}^3/\text{s}$ ,  $\dot{Q}=0.677 \text{ m}^3/\text{s}$  and  $\dot{Q}=0.94 \text{ m}^3/\text{s}$ . These air flows ensure the same velocity through the filter medium and give face velocities of  $U_0=0.99 \text{ m/s}$ ,  $1.88 \text{ m/s}$ ,  $2.61 \text{ m/s}$ , respectively.

The aerosol was supplied to the duct using a tube. Inside the duct, a probe with 4 outputs was used in order to achieve a uniform concentration of the aerosol inside the test-rig. During the test-rig calibration, particle measurements without filters were done in order to check their uniformity in the air flow, even though it is not possible to reach an isokinetic sampling due to the limitations in the lab. These limitations are e.g., the asymmetric distribution of the probes, the variations in the fan... Measurements confirmed that these deviations from the ideal case are not of relevant importance. As shown in the test-rig calibration, the aerosol concentration is stable in the test-rig; that is the reason why these deviations are not considered in the calculations.

The most representative figures obtained with the experiments are shown here.

## 4.1 Pressure drop

Pressure drop measurements were done for the tested filters at different air flows.

To perform these experiments, the manometer is placed to measure the pressure drop between the two sections just before and after the filter; thus it displays the pressure drop induced by the filter.

In this section, several graphs show the results of the pressure drop measurements. In all the graphs, the Y-axis refers to the pressure drop, in Pa, while the X-axis shows the air flow, in  $\text{m}^3/\text{s}$ .

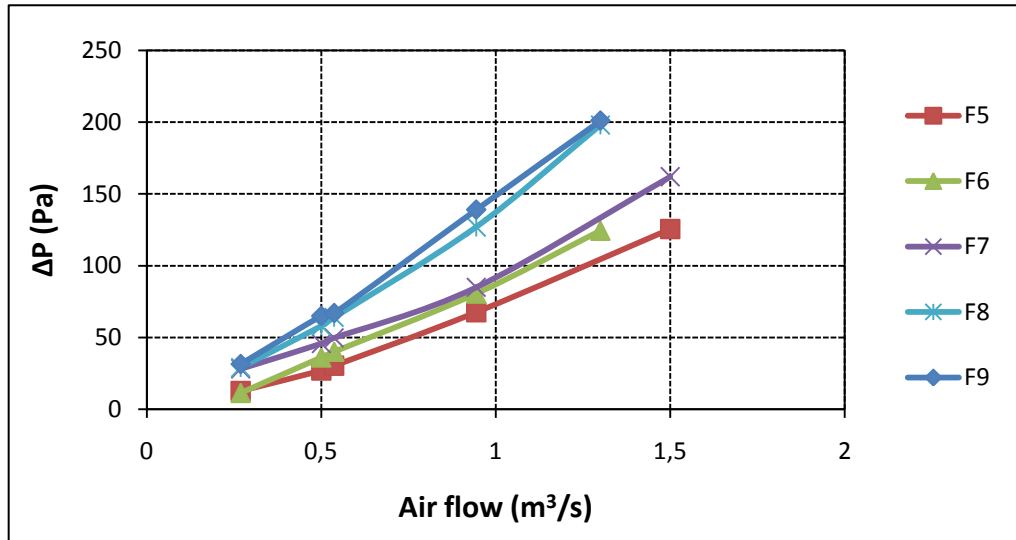


**Figure 4.1: Pressure drop for Charged Synthetic filters**

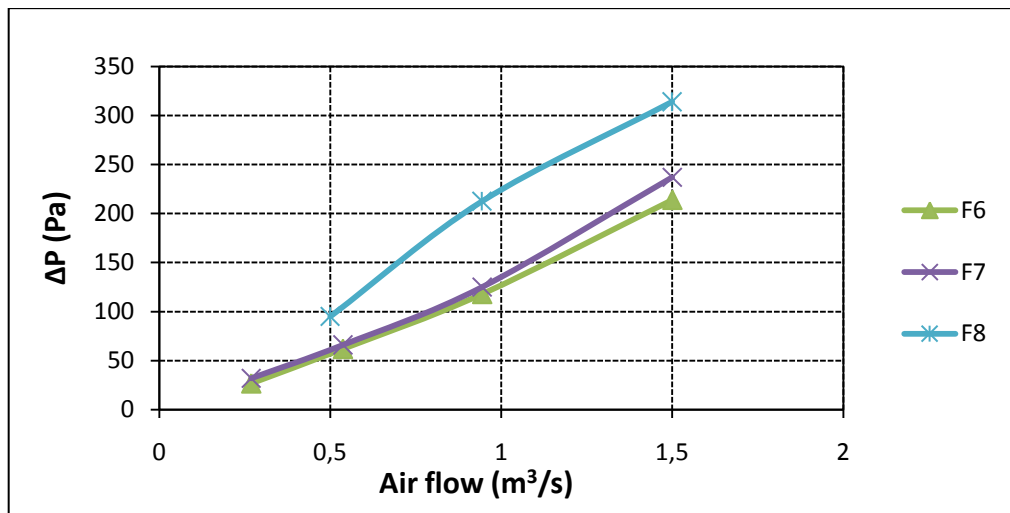


**Figure 4.2: Pressure drop for Glass Fiber filters**

Figures 4.1 and 4.2 show that, the higher the filter class, the higher the pressure drop. This is a fact in both charged synthetic and glass fiber filters. When the efficiency improves, the resistance to the air flow is increased. For higher air flows the difference in pressure drop is emphasized. Both figures show that the highest difference occurs between F7 and F8 filters. For glass fiber filters, this difference is increased due to the different size of F8 glass fiber filter. As the filtration area is smaller, the same air flow has a higher pressure drop.

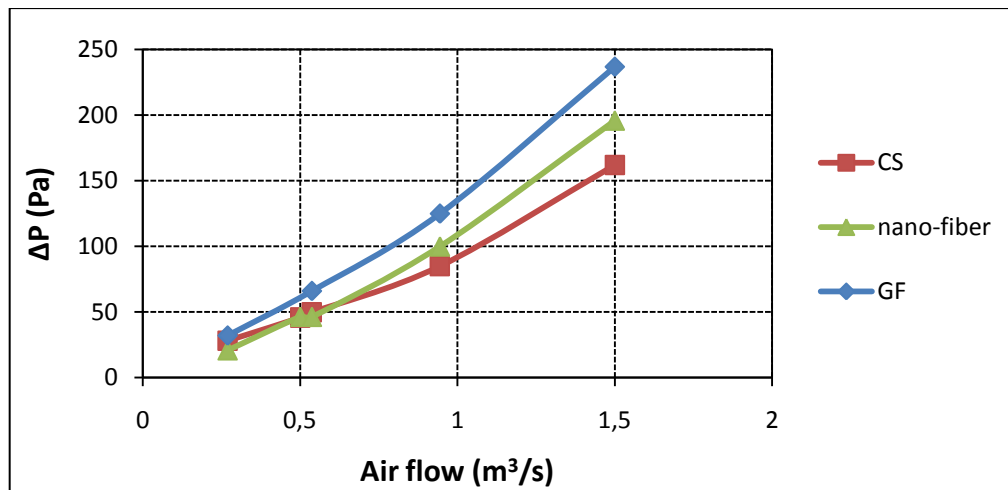


**Figure 4.3: Pressure drop for F7 filters**

Figure 4.3 summarizes the pressure drop of the three different F7 filters tested. The tested charged synthetic filter had a lower pressure drop than the glass fiber filter. The nano-fiber filter had an intermediate pressure drop, however, more similar to the one of the charged synthetic filter. This result agrees with the assumption made about the charge of the fibers in the nano-fiber filter. Figure 4.3 also shows that the difference in pressure drop increases with the air flow.

According to the experiments done, pressure drop increases with filter class and with air flow and the glass fiber filters had higher pressure drop than the charged synthetic filters. The conclusions are the same for the tested F6 and F8 filters.

## 4.2 Filtration efficiency

Filtration efficiency for different sizes is the cornerstone of this project. As mentioned before, the filtration efficiency has been calculated using the following expression:

$$E = 1 - \frac{C_{down}}{C_{up}}$$

For each experiment, the SMPS measured the concentration up and downstream, in order to compute the average efficiency. Each experiment was repeated five times and the average efficiency of the five efficiencies was calculated. All these experiments were performed using the neutralizer.

The standard deviation has been calculated for the different efficiencies in order to determine the accuracy of the obtained results. Expressions to calculate the standard deviation are summarized in appendix 8.2. The quality of the experiments is considered as acceptable if the standard deviations of the efficiencies are lower than 15%. This requirement is satisfied in almost all of the experiments.

Table 4.2-4.4 show the efficiencies achieved for the particle size of 400 nm, for the most penetrating particle size (MPPS) and the filtration efficiency for UFPs (<100 nm). These experiments were done with the DEHS aerosol and using the neutralizer.

**Table 4.2: Filtration efficiencies at 0.5 m<sup>3</sup>/s**

		E 400 nm	E MPPS	E UFPs
F5	CS	16%±2%	6%±4%	13%±6%
F6	CS	50%±5%	31%±3%	32%±5%
	GF	21±1%	17%±3%	23±2%
F7	CS	40%±3%	33%±2%	35%±1%
	GF	54%±1%	49%±2%	59%±2%
	nanofiber	43%±1%	35%±1%	35%±2%
F8	CS	66%±3%	43%±9%	46%±5%
	GF	67%±1%	57%±1%	62%±1%
F8 (0.34 m <sup>3</sup> /s)	GF	69%±4%	62%±2%	68%±4%
F9	CS	74%±3%	55%±2%	59%±4%

**Table 4.3: Filtration efficiencies at 0.944 m<sup>3</sup>/s**

		E 400 nm	E MPPS	E UFP
F5	CS	5%±3%	2%±0.2%	3%±2%
F6	CS	42%±4%	24%±5%	31%±6%
	GF	21%±1%	16%±2%	21%±1%
F7	CS	36%±2%	33%±3%	34%±3%
	GF	59%±2%	48%±2%	55%±3%
	nanofiber	41%±2%	36%±1%	36%±9%
F8	CS	51%±3%	37%±4%	38%±1%
	GF	69%±3%	53%±1%	56%±1%
F8 (0.68 m <sup>3</sup> /s)	GF	68% ±2%	55% ±1%	59% ±1%
F9	CS	72%±6%	54%±6%	56%±3%

**Table 4.4: Filtration efficiencies at 1.3 m<sup>3</sup>/s**

		E 400 nm	E MPPS	E UFP
F5	CS	5%±4%	2%±0.2%	3%±3%
F6	CS	38%±5%	20%±0.4%	27%±6%
	GF	22%±3%	13%±3%	21%±4%
F7	CS	37%±4%	32%±1%	34%±2%
	GF	58%±2%	46%±3%	51%±3%
	nanofiber	39%±1%	31%±3%	35%±2%
F8	CS	43%±3%	31%±1%	33%±2%
	GF	62%±1%	41%±3%	47%±1%
F8 (0.94 m <sup>3</sup> /s)	GF	69% ±3%	53% ±1%	56% ±1%
F9	CS	53%±1%	43%±5%	43%±2%

From Table 4.2-4.4, it is easy to see that filtration efficiency decreases with increasing flow rate. They also show how filtration efficiency increases with the filter class, as stated in the standards.

It is important to notice that, the efficiencies obtained may be underestimated because the air bypass was neglected. When doing the experiments, the filter frame was sealed to the duct so the bypass was minimized. For each filter, the sealing process was repeated until the test did not show any change of the filtration efficiency. This

ensures that there is an extremely low possibility that the efficiencies measured are underestimated.

The difference of MPPS between different kinds of filters was studied. Table 4.5 shows the sizes for the minimum efficiency obtained in the experiments.

**Table 4.5: Most Penetrating Particle Size (nm)**

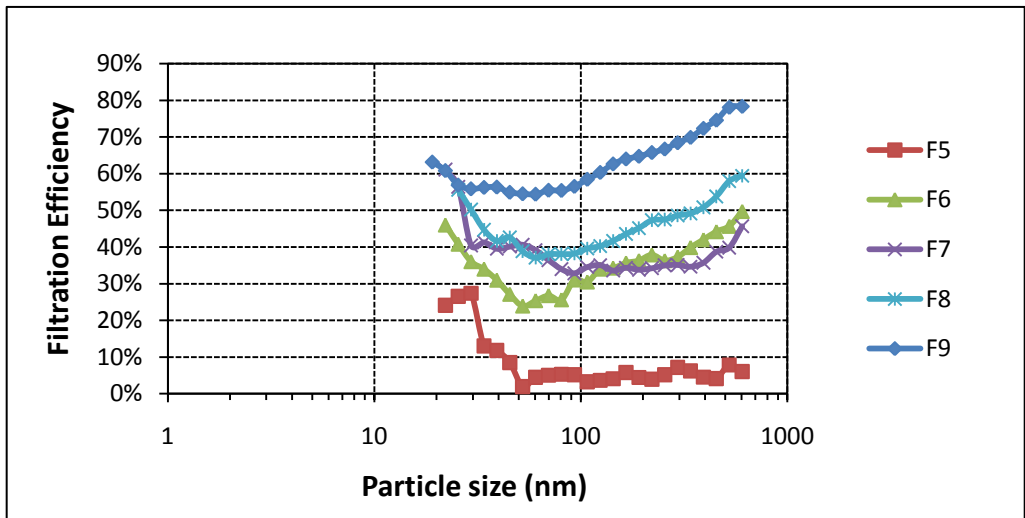
	Air flow	CS	GF	Nano-fiber
F5	0.5 m <sup>3</sup> /s	39.2	-	-
	0.944 m <sup>3</sup> /s	52.3	-	-
	1.3 m <sup>3</sup> /s	107.5	-	-
F6	0.5 m <sup>3</sup> /s	52.3	124.1	-
	0.944 m <sup>3</sup> /s	52.3	124.1	-
	1.3 m <sup>3</sup> /s	60.4	107.5	-
F7	0.5 m <sup>3</sup> /s	93.1	191.1	80.6
	0.944 m <sup>3</sup> /s	93.1	165.5	93.1
	1.3 m <sup>3</sup> /s	80.6	124.1	93.1
F8	0.34 m <sup>3</sup> /s	-	143.3	-
	0.5 m <sup>3</sup> /s	52.3	124.1	-
	0.68 m <sup>3</sup> /s	-	124.1	-
	0.944 m <sup>3</sup> /s	60.4	93.1	-
	1.3 m <sup>3</sup> /s	80.6	107.5	-
F9	0.5 m <sup>3</sup> /s	52.3	-	-
	0.944 m <sup>3</sup> /s	60.4	-	-
	1.3 m <sup>3</sup> /s	69.8	-	-

Table 4.5 shows that the MPPS is higher for glass fiber filters than that for charged synthetic filters. In general, the MPPS of glass fiber filters was found between 100 nm and 200 nm, while the MPPS for charged synthetic filters was lower than 100 nm. The size of minimum efficiency for the nano-fiber filter was similar to the one for charged synthetic filters. These results agree with the assumption of charged fibers in the nano-fiber filter. The MPPS range shows no important differences with the range stated in chapter 2.3.

Different graphs are presented in order to explain better the results. All the efficiency curves are presented with the filtration efficiency on the Y-axis and the particle size (nm), in logarithmic scale, on the X-axis. The advantage of a logarithmic scale is that different magnitudes can be represented in the same graph.

#### 4.2.1 Filter classes summary

The results of the efficiency determinations are presented in Table 4.2-4.4. In order to clearly compare filtration efficiencies, filter efficiency curves are also summarized in Figure 4.4-4.5 and in the appendix 8.3.



**Figure 4.4: Charged Synthetic filters at 0.159 m/s**

Figure 4.4 shows filtration efficiency for the five different charged synthetic filters tested at  $0.944 \text{ m}^3/\text{s}$ , which corresponds to an air velocity through the filter medium of  $0.159 \text{ m}^3/\text{s}$ . It can be seen how the filtration efficiency increases with the filter class. F9 is the most efficient filter while F5 is the least one.

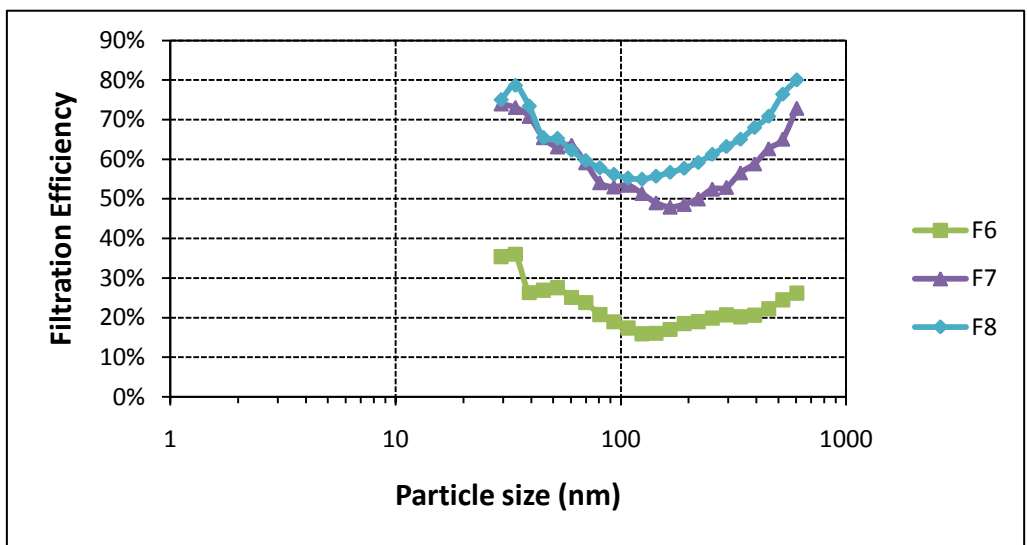


**Figure 4.5: Glass Fiber filters at 0.159 m/s**

Figure 4.5 shows the efficiency of glass fiber filters F6-F8 when the air velocity through the filter medium is  $0.159 \text{ m/s}$ . Tests for class F8 have been done at different air flows in order to compare them with the other filters at the same air velocity through the filter medium. In this case,  $0.159 \text{ m/s}$  is the velocity obtained when the air flow inside the duct is  $0.944 \text{ m}^3/\text{s}$ . These curves also show that filtration efficiency increases with filter class. Similar results for another two tested velocities are shown in appendix 8.3.

If the results presented in this section are compared with the expected ones showed in the theory, the consistency in the shape of the curves can be appreciated.

#### 4.2.2 Air flow influence

Several experiments were done in order to see the effect of the face velocity on the filtration efficiency. For each filter, the upstream and downstream particle concentration was measured at three different air flows.

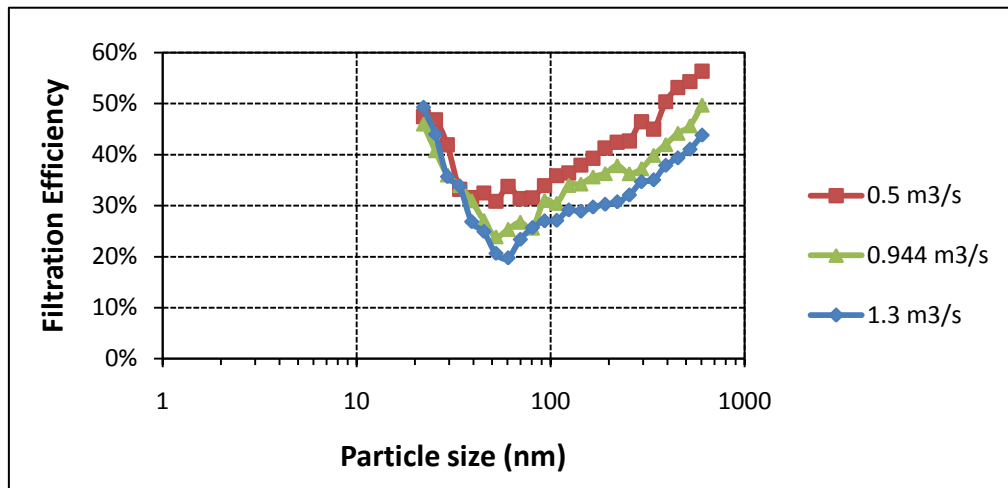


Figure 4.6: F6 Charged Synthetic filter at three air flow rates:  $0.5 \text{ m}^3/\text{s}$ ,  $0.944 \text{ m}^3/\text{s}$  and  $1.3 \text{ m}^3/\text{s}$

Figure 4.6 shows the efficiencies for F6 charged synthetic filters for the three different air flows tested. These experiments show that filtration efficiency increases when the air flow is reduced.

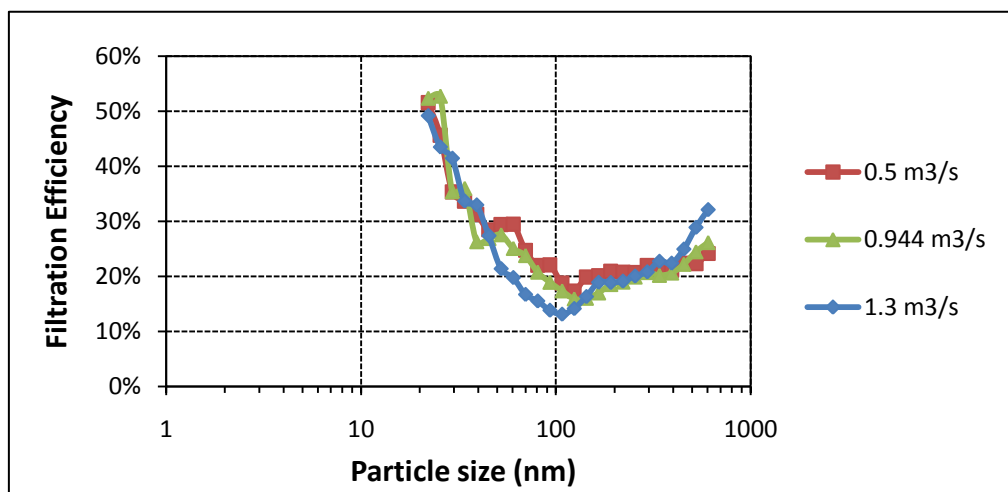


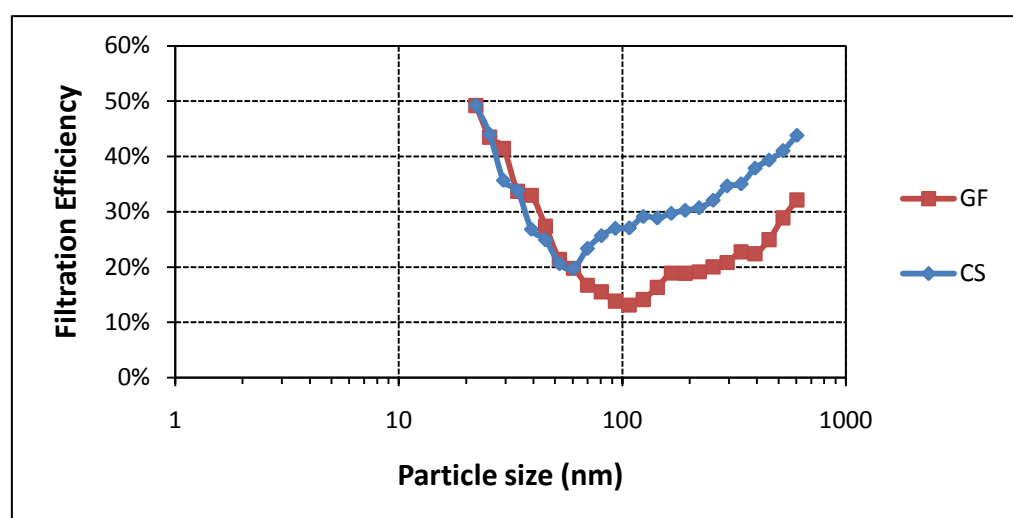
Figure 4.7: F6 Glass Fiber filter at three air flow rates:  $0.5 \text{ m}^3/\text{s}$ ,  $0.944 \text{ m}^3/\text{s}$  and  $1.3 \text{ m}^3/\text{s}$

Figure 4.7 depicts F6 glass fiber filter efficiency curves for three different air flows. They also indicate a slight decrease of particle capture when the air flow increases.

The main conclusion of these experiments is that the filtration efficiency is reduced if the air velocity is increased. This conclusion is independent of the filter media and filter class. The experimental results of F6 charged synthetic filter and glass fiber filter are presented here, but the conclusions can be extended to the other tested filters.

### 4.2.3 Filter media influence

The comparison between different filter media is also investigated, see Figures 4.8 and 4.9.



**Figure 4.8: Filtration efficiency of F6 filters at 1.3 m<sup>3</sup>/s: Glass Fiber (GF) filter and Charged Synthetic (CS) filter**

Figure 4.8 show the different filtration efficiencies of F6 charged synthetic and F6 glass fiber filters with the air flow rate of 1.3 m<sup>3</sup>/s. In the figure, the charged synthetic F6 filter has a higher particle collection than the glass fiber F6 filter. This result also appears for the experiments with the other air flows tested, but only one is shown here. The difference in the MPPS is also clear. The charged synthetic filters have their minimum efficiency at around 50-60 nm while the glass fiber filters MPPS is approximately between 110-120 nm.

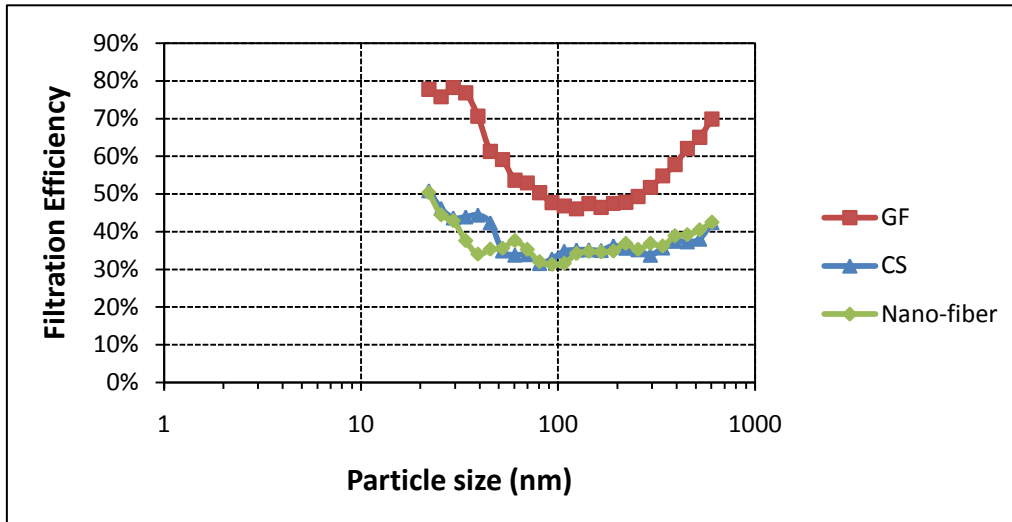


**Figure 4.9: Filtration efficiency of F7 filters at 1.3 m<sup>3</sup>/s: Glass Fiber (GF) filter, Charged Synthetic (CS) filter and Nano-fiber filter**

Figure 4.9 shows the performance of F7 glass fiber, charged synthetic and nano-fiber filters at 1.3 m<sup>3</sup>/s.

All the experiments done show similar performance of nano-fiber and charged synthetic filters, both in efficiency and in MPPS, but only the curves for 1.3 m<sup>3</sup>/s are presented here. These results support the assumption about charged fibers in the nano-fiber filter. The glass fiber filter of class F7 showed higher efficiency than the charged synthetic and nano-fiber filters of class F7 did. Nano-fiber filters are expected to have an enhanced efficiency but the experiments show that is not the most efficient option. The difference in the MPPS is not as clear as for F6 filters, but is still noticeable.

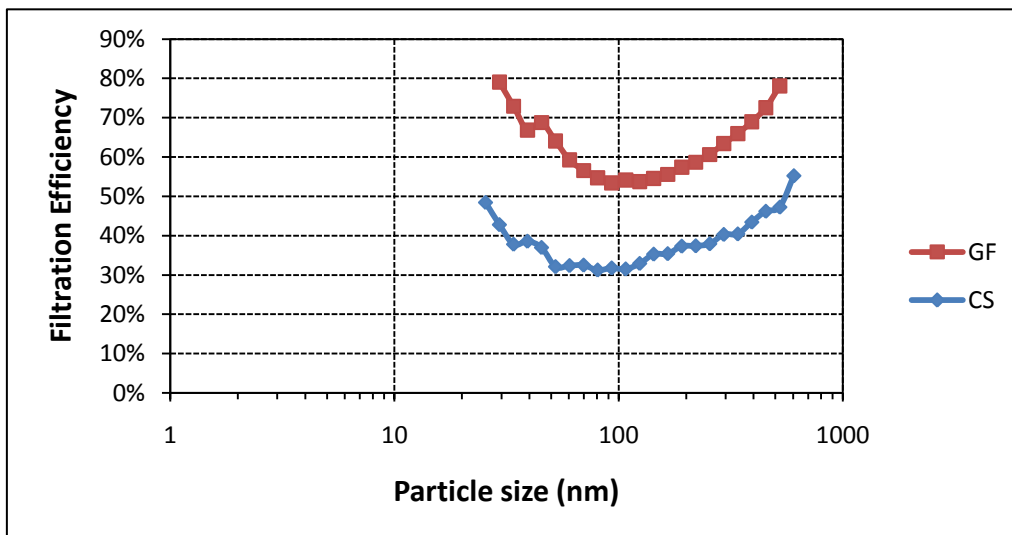


**Figure 4.10: Filtration efficiency of F8 filters at 0.219 m/s: Glass Fiber (GF) filter and Charged Synthetic (CS) filter**

Figure 4.10 shows the performance of F8 filters for the highest velocity tested. As for the F7 filters, the glass fiber filter showed better results than the charged synthetic F8

filter. The difference in the minimum efficiency size is less evident than for F6, but even so it is clear.

### 4.3 Neutralizer influence

All the results presented above were obtained when using the neutralizer. However, some experiments were also done without neutralizer. The differences between both experiments are shown in this section. It was already mentioned that, because the generated DEHS aerosol is probably not charged, the neutralizer charges it, theoretically with an equal number of negative and positive charges.

The results of these experiments are presented separately for each filter medium type, because they behave differently to charged particles. Only the results for F7 filters are shown in this section, but the same conclusions are reached with the other filter classes.

#### 4.3.1 Glass fiber filters

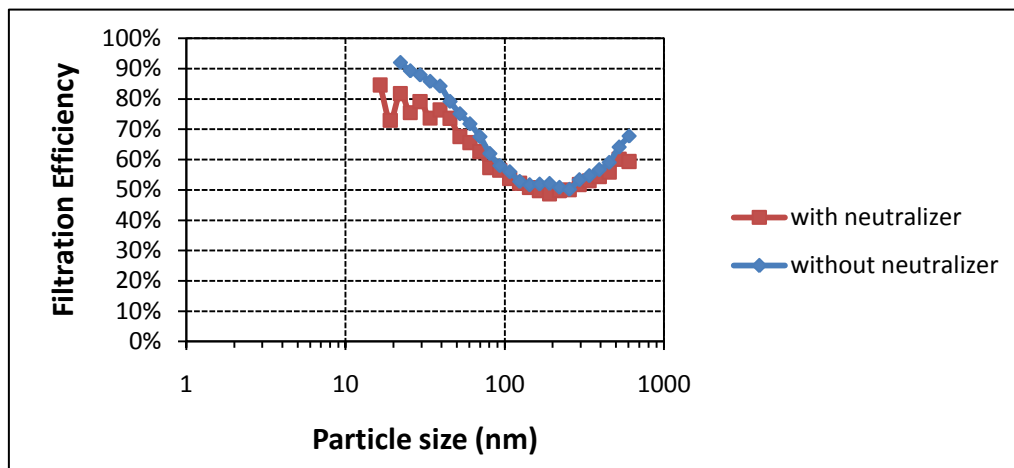


Figure 4.11: F7 Glass Fiber filter at 0.5 m<sup>3</sup>/s with and without neutralizer

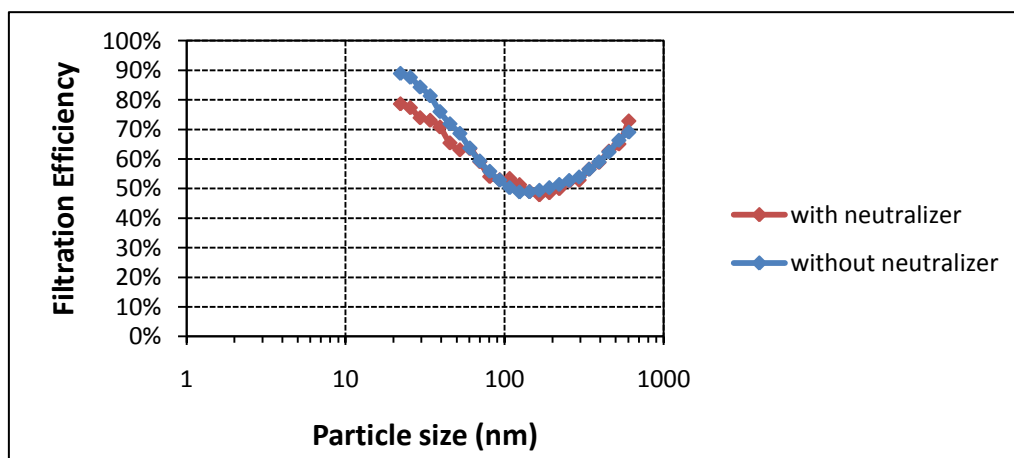
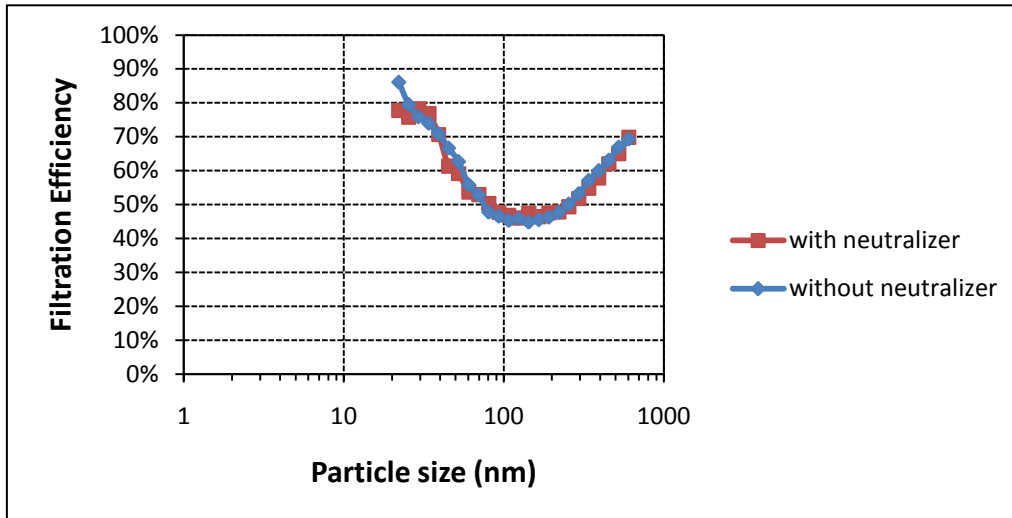


Figure 4.12: F7 Glass Fiber filter at 0.944 m<sup>3</sup>/s with and without neutralizer



**Figure 4.13: F7 Glass Fiber filter at 1.3 m<sup>3</sup>/s with and without neutralizer**

Figures 4.11, 4.12 and 4.13 show the different results for F7 glass fiber filter with and without neutralizer. As the fibers of this filter are not charged, there is no significant difference between both experiments; they do not act differently when filtering particles with different charge.

### 4.3.2 Charged Synthetic filters

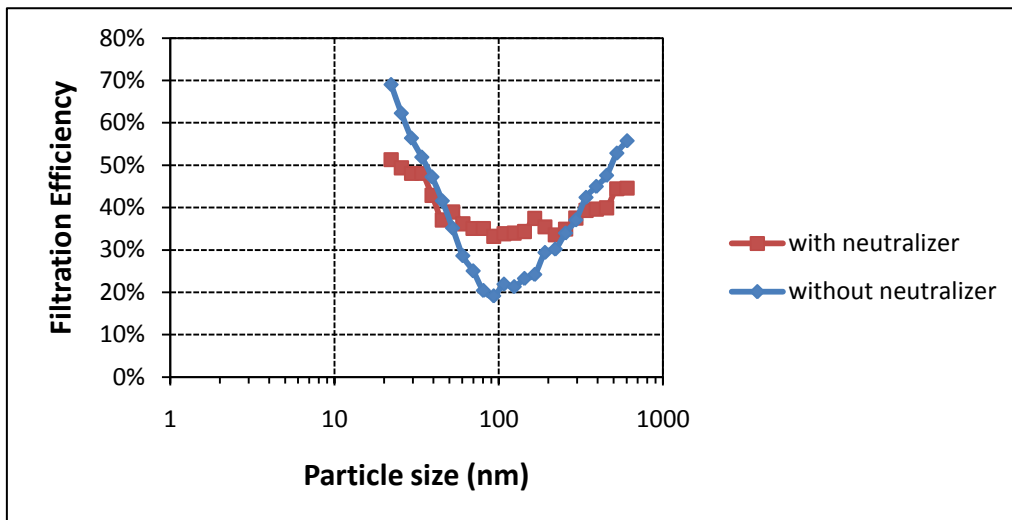


**Figure 4.14: F7 Charged Synthetic filter at 0.5 m<sup>3</sup>/s with and without neutralizer**

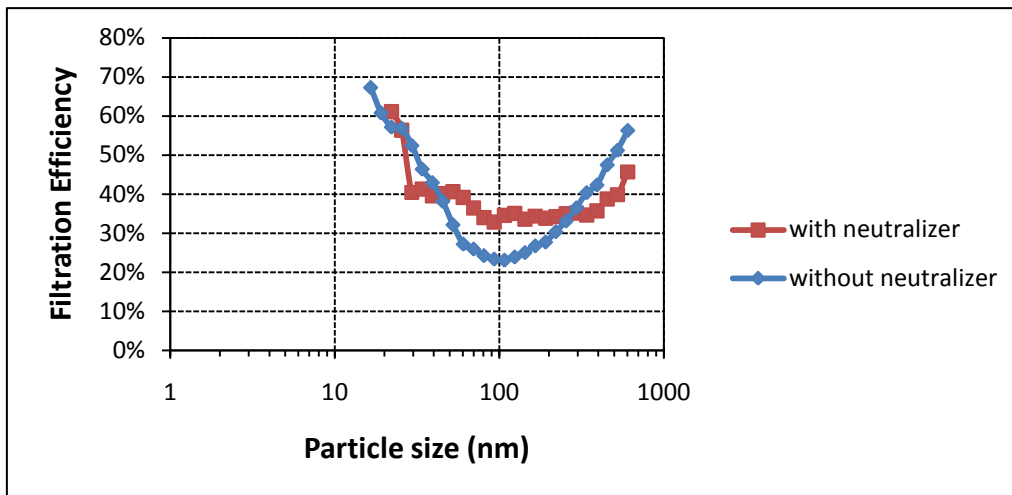


**Figure 4.15: F7 Charged Synthetic filter at 0.944 m<sup>3</sup>/s with and without neutralizer**

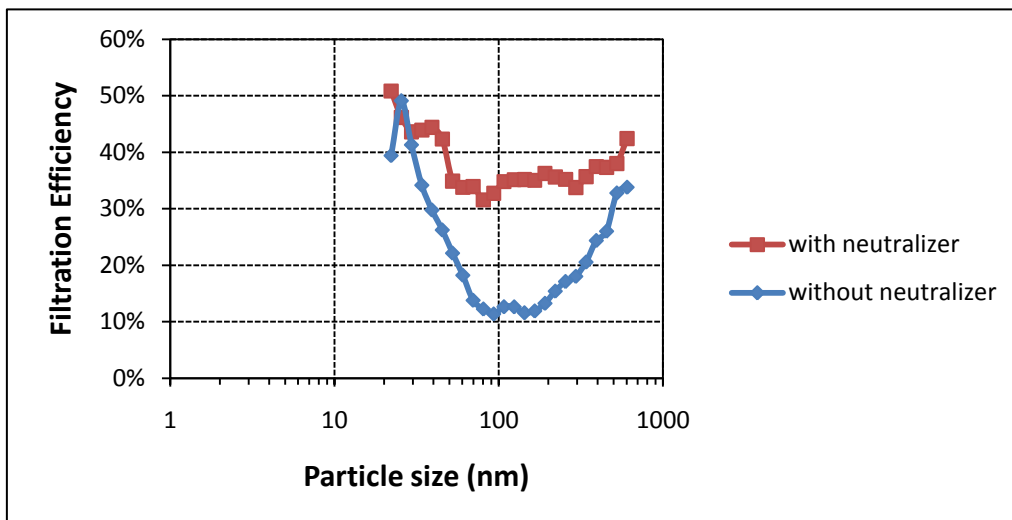


**Figure 4.16: F7 Charged Synthetic filter at 1.3 m<sup>3</sup>/s with and without neutralizer**

Figures 4.14, 4.15 and 4.16 show the experiments done for F7 charged synthetic filter. It can be appreciated that the efficiency of charged synthetic filters is increased when using the neutralizer. Figures 4.14 and 4.15 also show the opposite relationship for the very smallest and largest particles. The electrical charge level of the particles is increased when using the neutralizer, which reveals the advantages of the charged fibers.

### 4.3.3 Nano-fiber filters

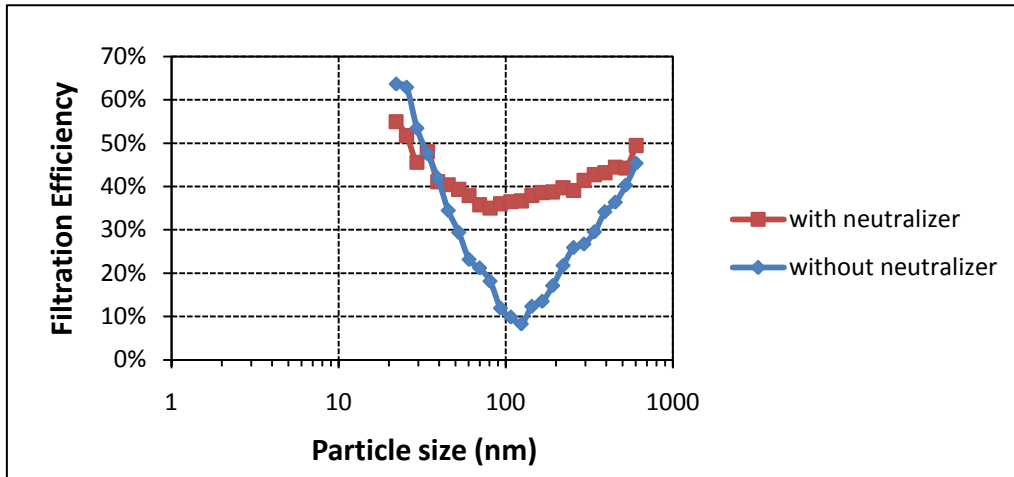


Figure 2.17: F7 Nano-fiber filter at 0.5 m<sup>3</sup>/s with and without neutralizer

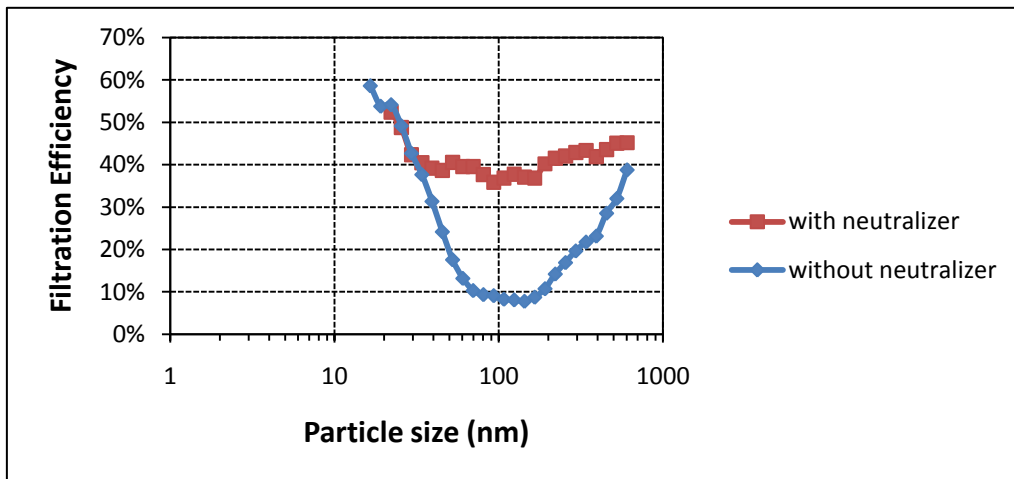


Figure 4.18: F7 Nano-fiber filter at 0.944 m<sup>3</sup>/s with and without neutralizer

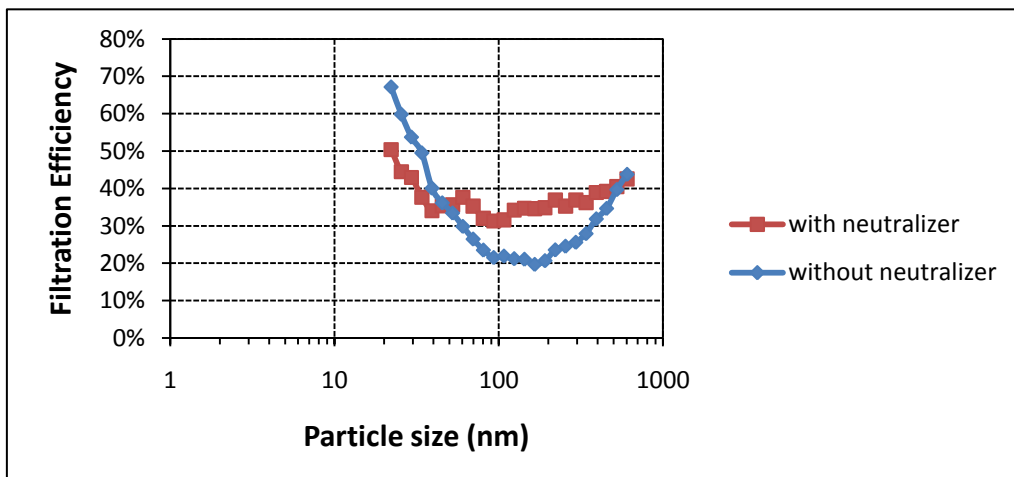


Figure 4.19: F7 Nano-fiber filter at 1.3 m<sup>3</sup>/s with and without neutralizer

Figures 4.17, 4.18 and 4.19 show the same experiments for F7 nano-fiber filter. They show that the aerosol charge level influences this kind of filter. Again, a similar behavior to that of charged synthetic filters is indicated.

Important conclusions can be reached with these experiments. Probably, charged synthetic filters tested by DEHS aerosol when it does not pass the neutralizer may predict their filtration efficiency after losing their electrical removal capacity.

#### 4.4 Aerosol influence

Additional experiments about filters tested by NaCl aerosol are also conducted in order to show the influence of the challenge aerosol. Two important reasons motivate these experiments: first, NaCl aerosol is commonly used for UFPs test; second, salt aerosol is the standard aerosol in the US standard ASHARE 52.2, while DEHS aerosol is prescribed in the European standard EN779.

The results were obtained with DEHS and NaCl aerosols passing the neutralizer. It is assumed that the initial generated DEHS has no charge while NaCl aerosol is charged.

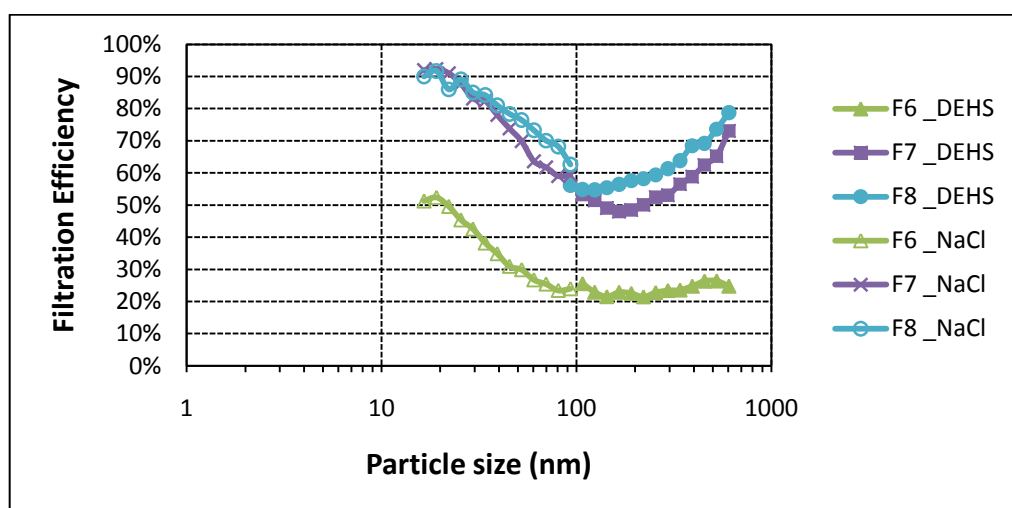


**Figure 4.20: DEHS and NaCl aerosols challenged Glass Fiber filters at 0.944 m<sup>3</sup>/s.**

Figure 4.20 shows the filtration efficiency for the different glass fiber filters tested with the two different aerosols: DEHS and NaCl. These experiments indicate that, when using glass fiber filters, the results are not influenced by the use of a neutralizer or charged particles.

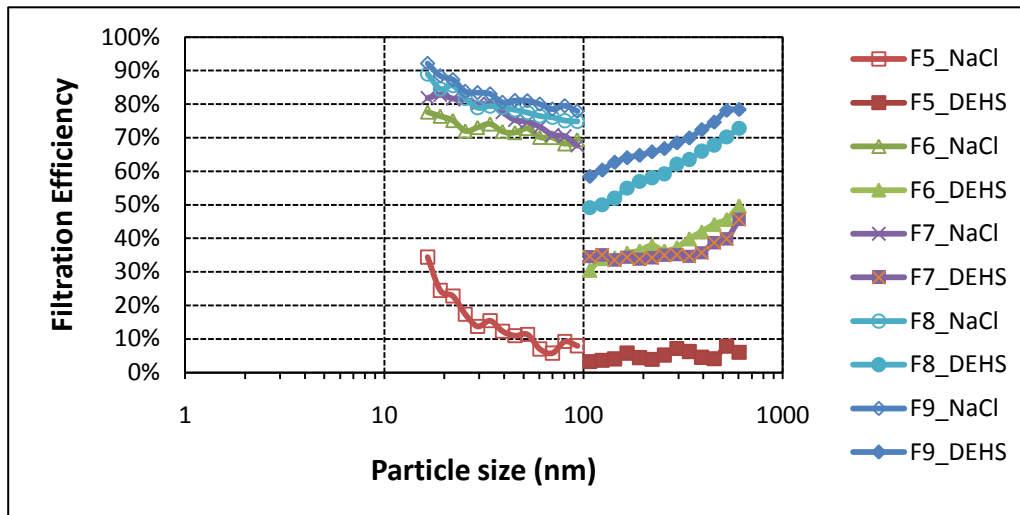


**Figure 4.21: DEHS and NaCl aerosols challenged Charged Synthetic filters at  $0.944 \text{ m}^3/\text{s}$**

Figure 4.21 shows the results of the same experiment, but for charged synthetic filters. The Figure shows how NaCl aerosol enhances the collection efficiency of charged synthetic filters. The main reason probably is that generated NaCl aerosol is much more charged than DEHS aerosol. Although, according to the manual, the used neutralizer should have enough capacity to neutralize the aerosols generated in the experiments, it may not have enough capacity to completely neutralize the highly charged NaCl aerosol.

Additionally, the tests with NaCl aerosol also show how charged synthetic filters improve their filtration efficiency when the challenged aerosol is charged.

## 5 Discussion and conclusions

Good air filtration can improve IAQ and, at the same time, reduce energy costs. SBS costs and illness cost due to poor air quality can be reduced by air filtering. Although filtration efficiency on UFPs is not the lowest one for particle filters, it is still meaningful to evaluate it due to its adverse health effects. Submicron particles are the ones filtered with less efficiency by commonly used filters; this fact, together with the hazards of submicron particles, makes the study of submicron particles become important.

It is commonly recommend using a filter of at least F7 class for most ventilation systems. If a lower filter class is used, it provides considerably less protection from this potentially dangerous type of air pollution, such as ultrafine and submicron particles. An important objective is to ensure that all the buildings satisfy this recommendation.

The experiments show the filtration efficiency for different filters and for different aerosols. F7 filters tested with a neutralized DEHS aerosol, at the nominal airflow rate  $0.944 \text{ m}^3/\text{s}$ , showed filtration efficiency values for UFPs in the range 34%-55%, depending on the filter media. The results of the experiments also showed that the filtration efficiency was substantially increased from F6 to F7 filters, while the pressure drop was not significantly amplified. The F8 and F9 filters showed UFPs efficiencies between 38% and 59%. However, the F8 and F9 filters had a substantially higher pressure drop than the F7 filters.

This study shows the performance of a group of commonly used bag filters in Sweden; hence, the study does not intend to extend the conclusions to all available filters in the market.

Working with lower flow rates increases slightly filtration efficiency. However, due to certain reasons, like energy costs and ventilation ducts size, it is not always possible to work with the most efficient flow rate.

The study shows that the experiments with/without neutralizer could induce important efficiency differences for charged synthetic filters, but negligible differences for glass fiber filters. These experiments also highlight the importance of using a neutralizer when testing charged synthetic filters. The two challenge aerosol experiments show how, in NaCl aerosol application, a high ability to neutralize is necessary. In this case, an unsuitable neutralizer can result in overestimation of the efficiency of charged synthetic filters.



## 6 Future works

It is important to investigate the advantages and disadvantages of used filters. This is a very interesting topic, due to the expected increase of efficiency in glass fiber filters, combined with the risk that these filters may release the collected particles. The effect of charged particles is another important field. Pressure drop and filtration efficiency overestimation due to non-uniformity fibers should also be studied carefully; the fibers are not 100% uniform and the pressure drop and filtration efficiency are calculated for uniform fibers.

Particle removal efficiency varies with the charge level in the challenged aerosol when using charged synthetic filters. It is interesting to further investigate the enhanced collection efficiency in order to increase IAQ.

The conclusions reached in the experiments with/without aerosol neutralization should be considered in future works: charged synthetic filters challenged by DEHS aerosol without neutralizer probably can predict their efficiency after losing their electrical removal capacity.

Air bypass can greatly reduce the real working efficiency of filters. In the experiments, the air bypass was neglected due to the results of filter test-rig calibration and the sealing process. In order to achieve a good IAQ, air bypass elimination and reduction is an important goal. Especially, air bypass should be considered when analyzing costs and benefits of air filtration. It is necessary to calculate the cost of reducing air bypass or to consider the reduction in performance due to air bypass [13].



## 7 References

- [1] W. J. Fisk, D. Faulkner, J. Palonen, O. Seppanen. *Indoor air 2002*: 12: 223-234. Performance and costs of particle air filtration technologies.
- [2] P.C. Raynor, B.G. Kim, G. Ramachandran, M.R. Strommen, J.H. Horns, A.J. Streifel. *Indoor air 2008*: 18: 51-62. Collection of biological and non-biological particles by new and used filters made from glass and electrostatically charged synthetic fibers.
- [3] Stephen N. Rudnick. *Aerosol Science and Technology*, 38:861-869, 2004. Optimizing the Design of Room Air Filters for the Removal of Submicrometer Particles.
- [4] J.T. Hanley, D.S. Ensor, D.D. Smith, L.E. Sparks. *Indoor air 1994*, 4: 169-178. Fractional Aerosol Filtration Efficiency of In-Duct Ventilation Air Cleaners.
- [5] Alan C. Veeck. January/February 2008. Air filtration: Guidelines and standards for using air filters.
- [6] David Matela. *HPAC Engineering*, June 2008. An inside look at air-filter selection.
- [7] R. Maus, H. Umhauer. *J. Aerosol Sci.* Vol 28, No 3, pp. 401-415, 1997. Collection efficiencies of coarse and fine dust filter media for airborne biological particles.
- [8] Lance A. Wallace, Steven J. Emmerich, Cynthia Howard-Reed. *Atmospheric Environment* 28, 2004 405-413. Effect of central fans and in-duct filters on deposition rates of ultrafine and fine particles in an occupied townhouse.
- [9] Lars E. Ekberg, Binbing Shi. Removal of ultrafine particles by ventilation air filters.
- [10] Bingbing Sh,I, Lars Ekberg, Sarka Langer. Removal of ultrafine particles and particles of the most penetrating size by new intermediate class filters.
- [11] P.S. Vinzents, P. Moller, M. Sorensen, L.E. Knudsen, O. Hertel, F. Palmgren Jensen, B. Schibye, S. Loft. *Environmental Health Perspectives*, volume 13 numer 11, November 2005. Personal exposure to ultrafine particles and oxidative DNA damage.
- [12] G. Bekö, G. Clausen, C.J. Weschler. *Building and environment* 43, 2008 1647-1657. Is the use of particle air filtration justified? Costs and benefits of filtration with regard to health effects, building cleaning and occupant productivity.
- [13] M. Ward, J. Siegel. Modeling filter bypass: impact on filter efficiency.
- [14] S. Rengasamy, B. C. Eimer. 2010. Total inward leakage of nanoparticles through filtering facepiece respirators.
- [15] W. C. Hinds. 1999. *Aerosol technology. Properties, behavior and measurements of airborne particles.*
- [16] Kun Li, Young Min Jo. June 2010. Dust collection by a fiber bundle electret filter in an MVAC system.
- [17] E. Abel, A. Elmroth. *Buildings and energy-a systematic approach.*
- [18] E. V. Bräuner, L. Forchhammer, P. Møller, J. Simonsen, M. Glasius, P. Wåhlin, O. Raaschou-Nielsen, S. Loft. August 2007. Exposure to Ultrafine Particles from ambient air and oxidative stress-induced DNA damage.
- [19] K. W. Lee, B. Y. H. Liu. February 2011. Experimental study of aerosol filtration by fibrous filters.
- [20] D. Matela. September 2007. Choosing the right air filter and filter media.

- [21] W. J. Fisk, D. Faulkner, J. Palonen, O. Seppanen. July 2003. Particle air filtration in HVAC supply-air streams.
- [22] V. Stone, H. Johnston, M. J. D. Clift. Air pollution, ultrafine and nanoparticle toxicology: Cellular and molecular interactions.
- [23] February 2003. Svensk standard SS-EN 779.
- [24] A. F. Sarofim, J. S. Lighty, E. G. Eddings. 2002. Fine particles: Health effects, characterization, mechanisms of formation, and modeling.
- [25] J Schwartz, L. M. Neas. January 2000. Fine particle are more strongly associated than coarse particles with acute respiratory health effects in schoolchildren.
- [26] I. Balásházy, W. Hofmann, T. Heistracher. January 2003. Local particle deposition patterns may play a key role in the development of lung cancer.
- [27] The Commtech Group. 2003. Achieving the desired indoor climate. Energy efficiency aspects of system design. Studentlitteratur.
- [28] k. Donaldson. 2002. Inflammation caused by particles and fibers. *Inhal Toxicol* 14:5-27
- [29] A. Nemmar, M.F. Hoylaerts, P.H. Hoet, B. Nemery. 2004. Possible mechanisms of the cardiovascular effects of inhaled particles: systemic translocation and prothrombotic effects.
- [30] R.P. Schins, J.H Lightbody, P.J. Borm, T. Shi, K. Donaldson, V. Stone. 2004. Inflammatory effects of coarse and fine particulate matter in relation to chemical and biological constituents.
- [31] L. Risom, M. Dybdahl, J. Bornholdt, U. Vogel, H. Wallin, P. Moller, et al. 2003a. Oxidative DNA damage and defence gene expression in the mouse lung after short-term exposure to diesel exhaust particles by inhalation. *Carcinogenesis* 24:1847-1852
- [32] L. Risom, P. Moller, U. Vogel, P.E.G. Kristjansen, S. Loft. 2003b. X-ray induced oxidative stress: DNA damage and gene expression of HO-1, ERCC1 and OGG1 in mouse lung. *Free Radic Res* 37:957-966.
- [33] D.M. Brown, V. Stone, P. Findlay, W. MacNee, K. Donaldson. 2000. Increased inflammation and intracellular calcium caused by ultrafine carbon black is independent of transition metals or other soluble compounds. *Occup. Environ Med* 57:685-691.
- [34] D.M. Brown, M.R. Wilson, W. MacNee, V. Stone, K. Donaldson. 2001. Size-dependent proinflammatory effects of ultrafine polystyrene particles: a role for surface area and oxidative stress in the enhanced activity of ultrafines. *Toxicol Appl Pharmacol* 175:191-199.
- [35] M. Dybdahl, L. Risom, P. Moller, H. Autrup, H. Wallin, U. Vogel, et al. 2003. DNA adduct formation and oxidative stress in colon and liver of Big Blue® rats after dietary exposure to diesel particles. *Carcinogenesis* 24:1759-1766.
- [36] A.M. Knaapen, P.J. Borm, C. Albrecht, R.P. Schins. 2004. Inhaled particles and lung cancer. Part A: Mechanisms. *Int J. Cancer* 109:779-809.
- [37] Matson, U. (2004). Ultrafine Particles in Indoor Air. Measurements and modeling. Göteborg: Chalmers University of Technology. Ph.D. Dissertation. ISBN/ISSN: 91-7291-522-6
- [38] E. Abt, H.H. Suh, P.J. Catalano, P. Koutrakis. 2000. Relative contribution of outdoor and indoor particle sources to indoor concentrations. *Environ Sci Technol* 34:3579-3587.

- [39] M. Dennekamp, S. Howarth, C.A.J. Dick, J.W. Cherrie, K. Donaldson, A. Seaton. 2001. Ultrafine particles and nitrogen oxides generated by gas and electric cooking. *Occup Environ Med* 58:511-516.
- [40] J.I. Levy, E.A. Houseman, L. Ryan, D. Richardson, J.D. Spengler. 2000. Particle concentrations in urban microenvironments. *Environ Health Perspect* 108:1051-1057.
- [41] C.M Long, H.H. Suh, P. Koutrakis. 2000. Characterization of indoor particle sources using continuous mass and size monitors. *J Air Waste Manag Assoc* 50:1236-1250.
- [42] H. Ozkaynak, J. Xue, J. Spengler, L. Wallace, E. Pellizzari, P. Jenkins. 1996. Personal exposure to airborne particles and metals: results from the Particle TEAM study in Riverside, California. *J Expo Anal Environ Epidemiol* 6:57-78.
- [43] B. Brunekreef, S.T. Holgate. 2002. Air pollution and health. *Lancet*: 360:1233-1242.
- [44] C.A. Pope, R.T. Burnett, M.J. Thun, E.E. Calle, D. Krewski, K. Ito, et al. 2002. Lung cancer, cardiopulmonary mortality, and long-term exposure to fine particulate air pollution. *JAMA* 287:1132-1141.



## 8 Appendix

### 8.1 Calibration of the filter test-rig

#### 8.1.1 Air velocity uniformity in the test duct

**Table 8.1: Air velocity upstream at 1.5 m<sup>3</sup>/s**

Point	1 <sup>st</sup> measure (m/s)	2 <sup>nd</sup> measure (m/s)	3 <sup>rd</sup> measure (m/s)	Mean value (m/s)
1	4.50	4.20	4.50	4.400
2	4.50	4.60	4.30	4.466
3	4.40	4.50	4.60	4.500
4	4.20	4.10	3.90	4.066
5	4.10	3.95	4.00	4.016
6	3.90	4.10	4.15	4.050
7	4.70	5.00	4.60	4.766
8	4.30	4.50	4.40	4.400
9	4.50	4.20	4.30	4.333
		Standard deviation	Mean value	Coefficient of variation
		0.248	4.333 m/s	0.0573

**Table 8.2: Air velocity upstream at 1 m<sup>3</sup>/s**

Point	1 <sup>st</sup> measure (m/s)	2 <sup>nd</sup> measure (m/s)	3 <sup>rd</sup> measure (m/s)	Mean value (m/s)
1	3.07	2.88	3.08	3.010
2	3.10	3.10	3.18	3.127
3	3.01	3.03	3.17	3.070
4	3.14	2.84	2.86	2.947
5	2.92	2.82	2.86	2.867
6	2.92	2.84	2.86	2.873
7	2.82	2.87	2.89	2.860
8	2.84	2.88	2.89	2.870
9	2.86	2.89	2.90	2.883
		Standard deviation	Mean value	Coefficient of variation
		0.101	2.945 m/s	0.0341

**Table 8.3: Air velocity upstream at 0.25 m<sup>3</sup>/s**

Point	1 <sup>st</sup> measure (m/s)	2 <sup>nd</sup> measure (m/s)	3 <sup>rd</sup> measure (m/s)	Mean value (m/s)
1	0.70	0.65	0.80	0.716
2	0.77	0.83	0.75	0.783
3	0.84	0.77	0.72	0.776
4	0.80	0.70	0.75	0.750
5	0.73	0.78	0.70	0.736
6	0.70	0.75	0.74	0.730
7	0.84	0.71	0.72	0.756
8	0.74	0.73	0.81	0.760
9	0.71	0.84	0.78	0.776
		Standard deviation	Mean value	Coefficient of variation
		0.0229	0.754 m/s	0.0304

**Table 8.4: Air velocity downstream at 1.5 m<sup>3</sup>/s**

Point	1 <sup>st</sup> measure (m/s)	2 <sup>nd</sup> measure (m/s)	3 <sup>rd</sup> measure (m/s)	Mean value (m/s)
1	4.50	4.40	4.50	4.466
2	4.10	4.05	4.15	4.100
3	4.30	4.30	4.50	4.366
4	4.50	4.90	4.70	4.700
5	5.00	5.00	4.10	4.700
6	4.50	4.60	4.40	4.500
7	4.50	4.3	4.50	4.433
8	4.40	4.60	4.60	4.533
9	4.30	4.30	4.40	4.333
		Standard deviation	Mean value	Coefficient of variation
		0.1861	4.459 m/s	0.0417

**Table 8.5: Air velocity downstream at 1 m<sup>3</sup>/s**

Point	1 <sup>st</sup> measure (m/s)	2 <sup>nd</sup> measure (m/s)	3 <sup>rd</sup> measure (m/s)	Mean value (m/s)
1	2.80	3.00	3.10	2.966
2	3.00	2.70	2.90	2.866
3	3.00	3.00	2.90	2.966
4	2.90	3.00	3.10	3.000
5	3.50	3.40	3.40	3.433
6	3.00	2.90	3.00	2.966
7	3.10	2.70	3.00	2.933
8	3.10	3.00	3.20	3.100
9	3.30	2.90	2.70	2.966
		Standard deviation	Mean value	Coefficient of variation
		0.1658	3.022 m/s	0.0548

**Table 8.6: Air velocity downstream at 0.25 m<sup>3</sup>/s**

Point	1 <sup>st</sup> measure (m/s)	2 <sup>nd</sup> measure (m/s)	3 <sup>rd</sup> measure (m/s)	Mean value (m/s)
1	0.90	0.90	0.90	0.900
2	0.80	0.80	0.90	0.833
3	0.80	0.90	0.90	0.866
4	1.09	0.97	1.00	1.020
5	1.00	1.00	1.00	1.000
6	0.90	0.90	0.90	0.900
7	0.85	0.90	0.90	0.883
8	0.85	0.90	0.85	0.866
9	0.80	0.90	0.85	0.850
		Standard deviation	Mean value	Coefficient of variation
		0.0650	0.902 m/s	0.0720

## 8.1.2 Aerosol uniformity in the test duct

**Table 8.7: Aerosol concentration 1,5 m<sup>3</sup>/s and 3 bar**

Point	1 <sup>st</sup> measure (particles/cm <sup>3</sup> )	2 <sup>nd</sup> measure (particles/cm <sup>3</sup> )	3 <sup>rd</sup> measure (particles/cm <sup>3</sup> )	Mean value (particles/cm <sup>3</sup> )
1	59800	59300	62300	60466.67
2	48200	48200	47900	48100
3	51900	52700	52700	52433.33
4	51000	50700	48600	50100
5	53500	54400	53900	53933.33
6	52600	53700	54100	53466.67
7	67000	71300	65400	67900
8	60500	60700	61200	60800
9	59500	60600	59500	59866.67
		Standard deviation	Mean value	Coefficient of variation
		6316.024	56340.74 particles/cm <sup>3</sup>	0.1121

**Table 8.8: Aerosol concentration 1 m<sup>3</sup>/s and 3 bar**

Point	1 <sup>st</sup> measure (part/cm <sup>3</sup> )	2 <sup>nd</sup> measure (part/cm <sup>3</sup> )	3 <sup>rd</sup> measure (part/cm <sup>3</sup> )	4 <sup>th</sup> measure (part/cm <sup>3</sup> )	5 <sup>th</sup> measure (part/cm <sup>3</sup> )	Mean value (part/cm <sup>3</sup> )
1	79400	84300	81700	104000	93600	88600
2	68200	66900	66100	76700	71900	69960
3	74100	74600	74000	77100	77400	75440
4	72100	73100	69100	83700	87800	77160
5	75300	75600	77100	83100	87300	79680
6	73800	74400	74300	82200	77200	76380
7	99100	85200	87000	71000	112000	90860
8	87100	87200	89300	94500	99100	91440
9	84700	84000	84800	109000	86800	89860
		Standard deviation	Mean value		Coefficient of variation	
		8071.004	82153.33 particles/cm <sup>3</sup>		0.098243	

**Table 8.9: Aerosol concentration 0.25 m<sup>3</sup>/s and 3 bar**

Point	1 <sup>st</sup> measure (particles/cm <sup>3</sup> )	2 <sup>nd</sup> measure (particles/cm <sup>3</sup> )	3 <sup>rd</sup> measure (particles/cm <sup>3</sup> )	Mean value (particles/cm <sup>3</sup> )
1	217000	223000	215000	218333.3
2	190000	197000	188000	191666.7
3	185000	199000	202000	195333.3
4	177000	212000	211000	200000
5	181000	228000	225000	211333.3
6	175000	214000	217000	202000
7	176000	219000	225000	206666.7
8	188000	233000	236000	219000
9	181000	226000	236000	214333.3
		Standard deviation	Mean value	Coefficient of variation
		9926.271	206518.5 particles/cm <sup>3</sup>	0.048065

### 8.1.3 Maximum aerosol concentrations in the experiments

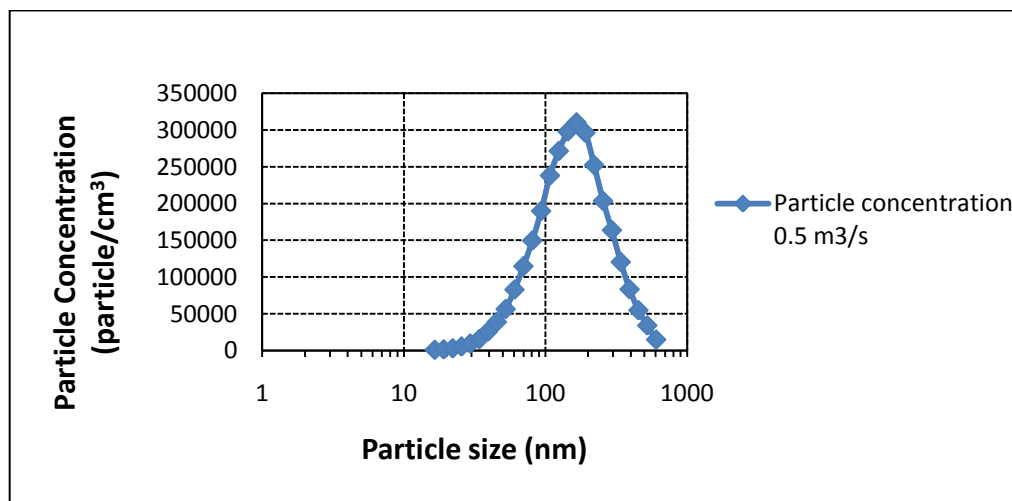


**Figure 8.1: Particle concentration at 0.5 m<sup>3</sup>/s**

### 8.1.4 Zero % efficiency test

**Table 8.10: Efficiency with no filter**

Measuring point	Concentration (particles/cm <sup>3</sup> )	Efficiency
Upstream	10200	
Downstream	9651	-2.1%
Upstream	8700	
Upstream	82600	
Downstream	75100	0.7%
Upstream	68700	
Upstream	114000	
Downstream	104000	1.7%
Upstream	97500	
Upstream	75800	
Downstream	70600	-0.1%
Upstream	65300	
Upstream	98700	
Downstream	92200	-0.8%
Upstream	84300	

### 8.1.5 Aerosol generator stability

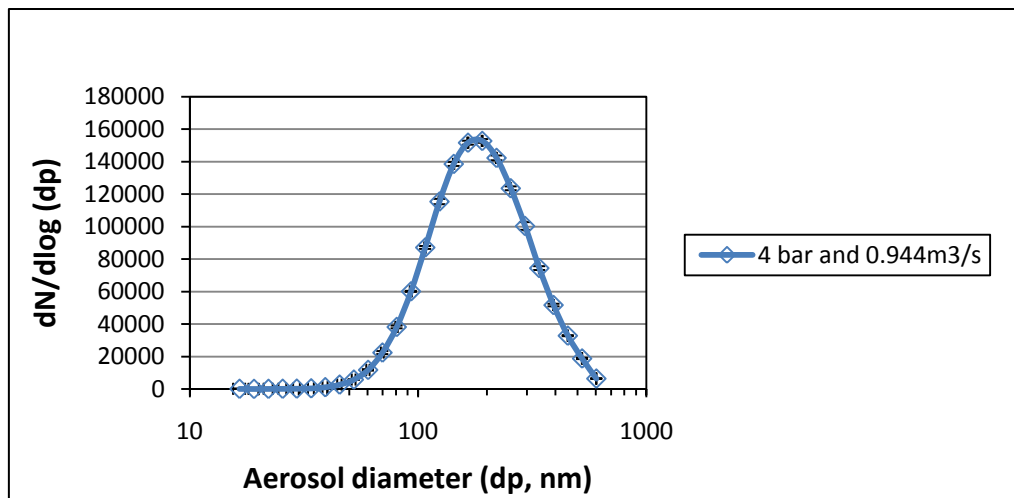


**Figure 8.2: Aerosol generator stability under 4 bar and at 0.944 m<sup>3</sup>/s**

## 8.1.6 Filter test-rig under over-pressure

**Table 8.11: Over-pressure checking at 0.25 m<sup>3</sup>/s**

0.25 m <sup>3</sup> /s		1 <sup>st</sup> measurement	2 <sup>nd</sup> measurement	3 <sup>rd</sup> measurement
Section 1	1	0.3 Pa	0.3 Pa	0.3 Pa
	2	0.3 Pa	0.3 Pa	0.3 Pa
	3	0.4 Pa	0.4 Pa	0.4 Pa
Section 2		0.4 Pa	0.4 Pa	0.5 Pa
Section 3	1	0.5 Pa	0.5 Pa	0.6 Pa
	2	0.6 Pa	0.6 Pa	0.6 Pa
	3	0.4 Pa	0.4 Pa	0.4 Pa

**Table 8.12: Over-pressure at 1.5 m<sup>3</sup>/s**

1.5 m <sup>3</sup> /s		1 <sup>st</sup> measurement	2 <sup>nd</sup> measurement	3 <sup>rd</sup> measurement
Section 1	1	13.5 Pa	13.6 Pa	13.5 Pa
	2	9.5 Pa	10.2 Pa	9.9 Pa
	3	11.6 Pa	12.4 Pa	11.9 Pa
Section 2		13.9 Pa	13.7 Pa	13.5 Pa
Section 3	1	12.9 Pa	12.4 Pa	12.6 Pa
	2	14.6 Pa	15.1 Pa	15.0 Pa
	3	11.4 Pa	11.1 Pa	11.1 Pa

## 8.2 Standard deviation methods

Two expressions were used in order to calculate the standard deviation of the filtration efficiencies obtained. The first one is the general one for the calculation of standard deviation, while the second one is the one used for the cases where five consecutive measurements were taken up and downstream and filtration efficiency was calculated with the average concentrations instead of using the average of the different efficiencies.

$$S_x = \sqrt{\frac{1}{n-1} \sum_{i=1}^n (x_i - \bar{x})^2}$$

where  $n$  is the number of samples,  $x_i$  is the efficiency for each sample and  $\bar{x}$  is the average value.

$$S_x = \sqrt{\left(\frac{S_{down}}{C_{down}}\right)^2 + \left(\frac{S_{up}}{C_{up}}\right)^2} \times E$$

where  $S_{down}$  and  $S_{up}$  are the standard deviations of the measurements downstream and upstream, respectively,  $C_{down}$  and  $C_{up}$  are the mean values of the measurements downstream and upstream, respectively and  $E$  is the filtration efficiency obtained.

### 8.3 Additional results

Figure 8.3-8.6 shows the results from filter tests carried out using the DEHS aerosol with neutralizer.

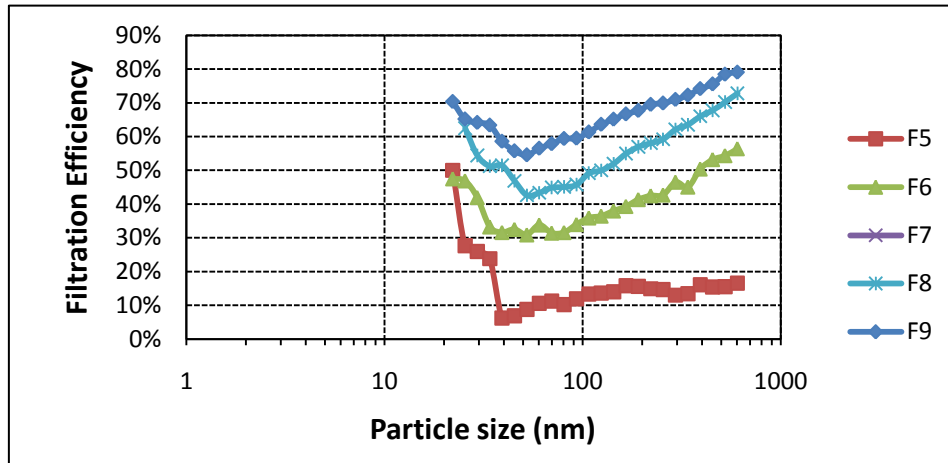


Figure 8.3: Charged Synthetic filters at 0.084 m/s

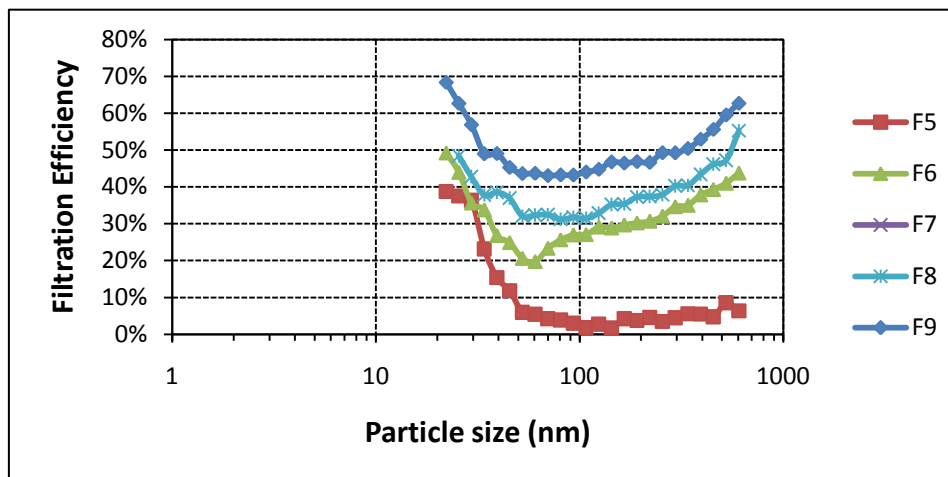
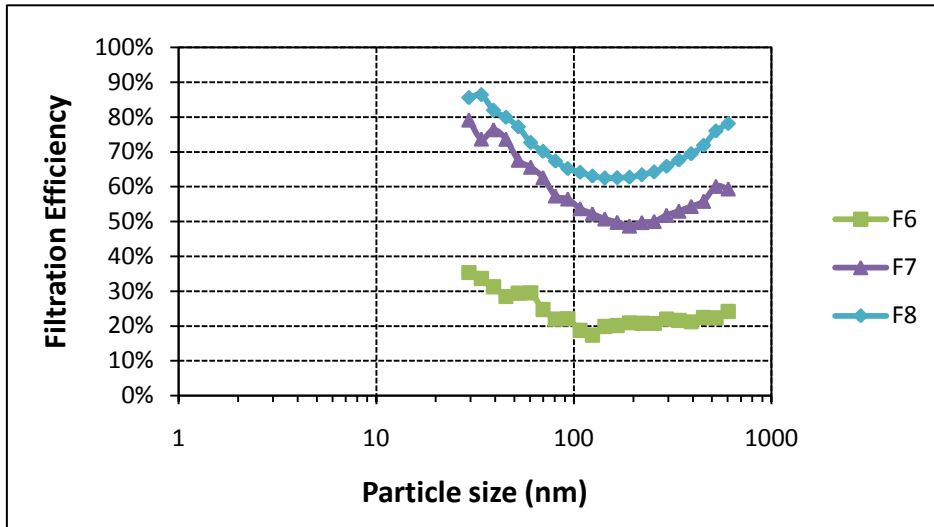
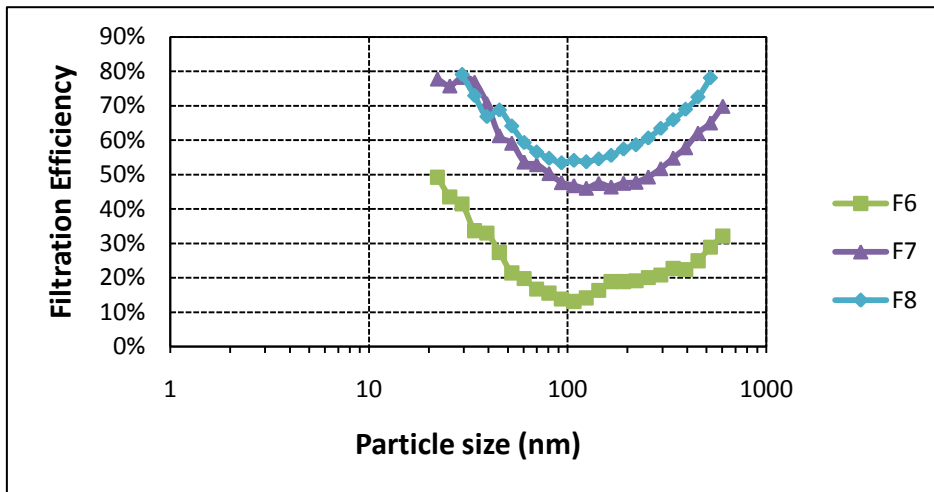


Figure 8.4: Charged Synthetic filters at 0.219 m/s



**Figure 8.5: Glass Fiber filters at 0.084 m/s**



**Figure 8.6: Glass Fiber filters at 0.219 m/s**